

See discussions, stats, and author profiles for this publication at: <https://www.researchgate.net/publication/263099813>

7-MEOTA-donepezil like compounds as cholinesterase inhibitors: Synthesis, pharmacological evaluation, molecular modeling and QSAR studies

ARTICLE *in* EUROPEAN JOURNAL OF MEDICINAL CHEMISTRY · MAY 2014

Impact Factor: 3.45 · DOI: 10.1016/j.ejmech.2014.05.066 · Source: PubMed

CITATIONS

9

READS

52

15 AUTHORS, INCLUDING:



Kamil Musilek

University of Hradec Králové

189 PUBLICATIONS 1,846 CITATIONS

SEE PROFILE



Veronika Opletalová

Charles University in Prague

55 PUBLICATIONS 551 CITATIONS

SEE PROFILE



Daniela Ripova

Prague Psychiatric Center

93 PUBLICATIONS 414 CITATIONS

SEE PROFILE



Kamil Kuca

University hospital Hradec Kralove

592 PUBLICATIONS 5,945 CITATIONS

SEE PROFILE



Original article

7-MEOTA–donepezil like compounds as cholinesterase inhibitors: Synthesis, pharmacological evaluation, molecular modeling and QSAR studies



Jan Korabecny^{a, b}, Rafael Dolezal^a, Pavla Cabelova^d, Anna Horova^b, Eva Hrubá^d, Jan Ricny^e, Lukas Sedlacek^g, Eugenie Nepovimova^{a, b}, Katarina Spilovska^{a, b}, Martin Andrs^{a, b}, Kamil Musilek^f, Veronika Opletalova^d, Vendula Sepsova^{a, b}, Daniela Ripova^e, Kamil Kuca^{a, b, c, f, *}

^a Biomedical Research Centre, University Hospital Hradec Kralove, Sokolska 581, 500 05 Hradec Kralove, Czech Republic

^b Department of Toxicology, Faculty of Military Health Sciences, University of Defence, Trebesska 1575, 500 01 Hradec Kralove, Czech Republic

^c Centre for Advanced Studies, Faculty of Military Health Sciences, University of Defence, Trebesska 1575,

500 01 Hradec Kralove, Czech Republic

^d Department of Pharmaceutical Chemistry and Drug Control, Faculty of Pharmacy in Hradec Kralove, Charles University in Prague, Heyrovského 1203, 500 05 Hradec Kralove, Czech Republic

^e Laboratory of Biochemistry and Brain Pathophysiology and AD Center, Prague Psychiatric Center, Ustavní 91, 181 03 Prague 8, Czech Republic

^f Department of Chemistry, Faculty of Science, University of Hradec Kralove, Rokitanského 62, 500 03 Hradec Kralove, Czech Republic

^g Department of Anthropology and Human Genetics, Faculty of Science, Charles University in Prague, Vinicna 7, 128 43 Prague, Czech Republic

ARTICLE INFO

Article history:

Received 29 March 2014

Received in revised form

4 May 2014

Accepted 26 May 2014

Available online xxx

Keywords:

Alzheimer's disease

Tacrine

7-MEOTA

AChE/BChE inhibitors

Molecular modeling

QSAR

ABSTRACT

A novel series of 7-methoxytacrine (7-MEOTA)–donepezil like compounds was synthesized and tested for their ability to inhibit electric eel acetylcholinesterase (*EeAChE*), human recombinant AChE (*hAChE*), equine serum butyrylcholinesterase (*eqBChE*) and human plasmatic BChE (*hBChE*). New hybrids consist of a 7-MEOTA unit, representing less toxic tacrine (THA) derivative, connected with analogues of *N*-benzylpiperazine moieties mimicking *N*-benzylpiperidine fragment from donepezil. 7-MEOTA–donepezil like compounds exerted mostly non-selective profile in inhibiting cholinesterases of different origin with IC₅₀ ranging from micromolar to sub-micromolar concentration scale. Kinetic analysis confirmed mixed-type inhibition presuming that these inhibitors are capable to simultaneously bind peripheral anionic site (PAS) as well as catalytic anionic site (CAS) of AChE. Molecular modeling studies and QSAR studies were performed to rationalize studies from *in vitro*. Overall, 7-MEOTA–donepezil like derivatives can be considered as interesting candidates for Alzheimer's disease treatment.

© 2014 Elsevier Masson SAS. All rights reserved.

1. Introduction

Acetylcholinesterase (AChE, E.C. 3.1.1.7) and butyrylcholinesterase (BChE; E.C. 3.1.1.8) are important and widely distributed enzymes. AChE acts primarily as a regulatory enzyme at cholinergic synapses, while BChE functions as a non-specific hydrolase involved in scavenging for anticholinesterases, including organophosphates [1]. These enzymes have gained particular interest because they are targets for Alzheimer's disease (AD)

treatment. As AD progresses, the level of AChE decreases, while that of BChE remains unchanged or slightly increased in the temporal cortex and hippocampus [2]. The relation between the observed cholinergic dysfunction and AD severity provided a rationale for the therapeutic use of AChE inhibitors (AChEIs), such as tacrine, donepezil, galantamine and rivastigmine (Fig. 1) [3]. Apart from AChEIs, *N*-methyl-*D*-aspartate antagonist memantine have been approved by U.S. Food and Drug Administration (FDA) for the treatment of moderate to severe AD [4]. Due to an unknown etiology of the disease, many therapeutic strategies have emerged. Among them, therapeutic strategies aimed at deposits of aberrant proteins namely β -amyloid (A β) and τ -protein, oxidative stress, mitochondrial abnormalities and neuroinflammatory processes

* Corresponding author. Centre for Advanced Studies, Faculty of Military Health Sciences, University of Defence, Trebesska 1575, 500 01 Hradec Kralove, Czech Republic.

E-mail address: kamil.kuca@fnhk.cz (K. Kuca).

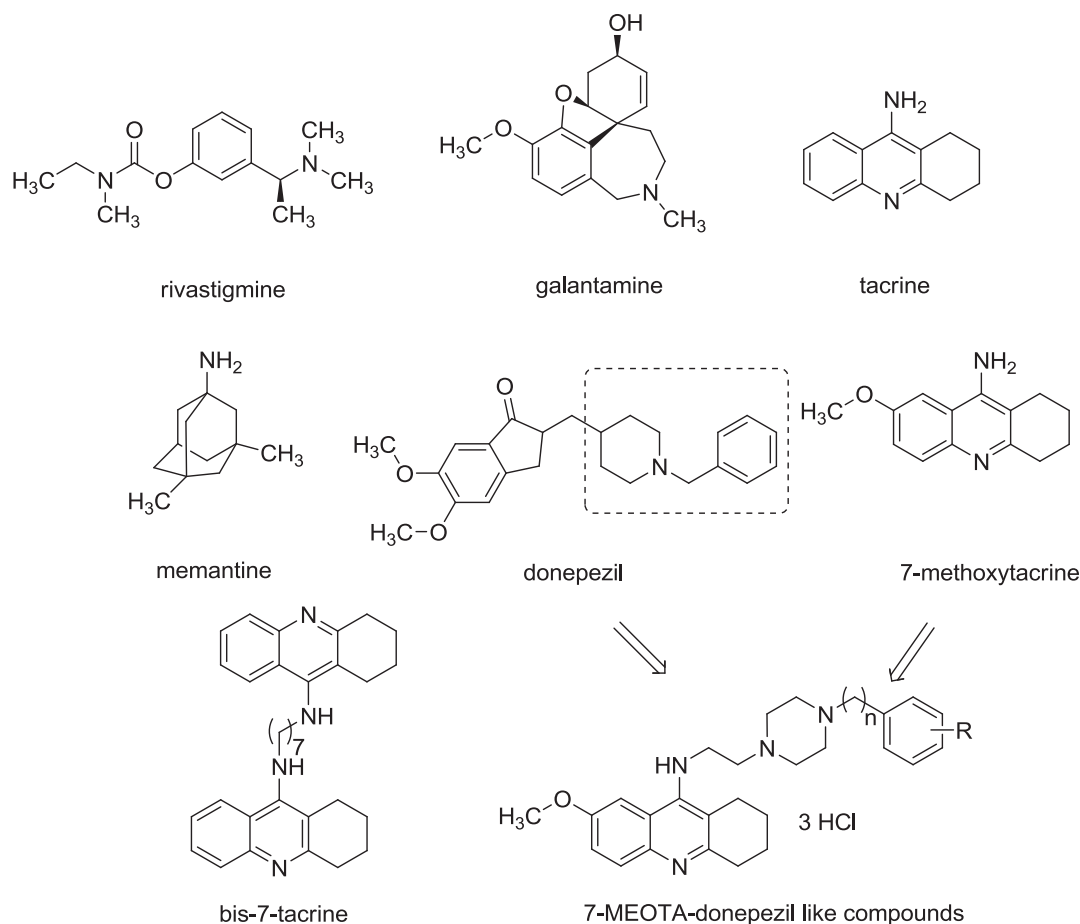


Fig. 1. Structures of AChEIs, NMDA-receptor antagonist memantine and novel class of 7-MEOTA–donepezil like compounds for the treatment of AD.

represent the field of interest in AD research [5,6]. Whilst all the proposed therapeutic approaches are failing, development of new AChEIs remains at the forefront of scientific efforts [7,8].

Being the first drug approved for AD treatment by the FDA, tacrine (1,2,3,4-tetrahydroacridin-9-amine, THA) is a non-selective and non-competitive reversible inhibitor of both AChE and BChE. Besides the use in palliative care, THA displays side effects that include hepatotoxicity and gastrointestinal problems [9]. To improve its pharmacological profile, several molecular modifications have been adopted [10]. 7-Methoxytacrine (7-MEOTA, Fig. 1) was developed in the Czech Republic as a new therapeutic for AD treatment [11]. As a centrally active AChEI, it was found capable of protection against incapacitating agent 3-quinclidinyl benzilate (BZ compound) [12]. In addition, 7-MEOTA is pharmacologically equal to THA and more importantly, less toxic [13]. Donepezil (1-benzyl-4-[5,6-dimethoxy-(1-indanone)-2-yl]methylpiperidine hydrochloride), also known as E2020, was found to be highly selective AChE inhibitor [14]. The efficacy of donepezil was evaluated in phase II and III trials with more than 1000 volunteers resulting in improvement of memory decline in AD patients with no signs of hepatotoxicity. Based on these results, donepezil was approved by FDA in 1996 for the treatment of mild to moderate AD [15]. Donepezil is recognized by AChE active site by interactions with benzyl moiety (catalytic anionic site (CAS) of AChE), the nitrogen atom of the piperidine (mid-gorge) and dimethoxyindanone moiety (peripheral anionic site (PAS) of AChE) [16].

Notably, the hybrid molecule approach in which two distinct pharmacological (and chemical) classes of compounds are connected covalently in one molecule has been successfully applied to

the design of anti-dementia agents [17,18]. In this context, major efforts have been devoted to the development of the so-called “dual binding site” AChEIs. By simultaneously interacting with AChE CAS and PAS, these AChEIs might mitigate the cognitive deficit in AD by restoring cholinergic activity. Moreover, these compounds can reduce A β burden acting as disease modifying agents, since direct interaction between compound and PAS of AChE is involved into retardation of A β assembly [19]. Based on this presumption, bis-7-THA (Fig. 1) was developed as the first agent able to simultaneously interact with both parts of AChE and more importantly, being 1000-fold more potent AChEI than THA itself [20]. Examples of newly prepared THA-based heterodimer families include the combination of THA with structural units such as tacrine–huperzine A [21], tacrine–indole [22], tacrine-4-oxo-4*H*-chromene [23] and tacrine–propidium [24].

In continuation with our research for new cholinesterase inhibitors (ChEIs) based on less toxic THA derivative [17,25–27], 7-MEOTA, in the present study we describe novel class of 7-MEOTA–donepezil like compounds (Fig. 1) as inhibitors of human (*hAChE*, *hBChE*) and animal (electric eel AChE, *EeAChE*; equine BChE, *eqBChE*) cholinesterases (ChEs). The fact that THA and/or 7-MEOTA scaffold could interact within CAS as well as PAS [28] regions of AChE together with the previously described statement that *N*-benzylpiperidine [16] or its isostere *N*-benzylpiperazine [29,31] moieties are truly CAS ligands, led us to assumption that such combination might bring enhancement in term of ChE inhibition. Very similar strategy was reported earlier by Alonso and co-workers [32], however, exploiting acridine or 6-chlorotacrine as CAS ligand in connection with indanone or phthalimide acting as

peripheral site ligands. Additionally, we also synthesized 7-MEOTA–piperazine derivatives attached to phenyl ring by different alkyl linkers and investigated the substitution by some aliphatic residues. Finally, we used the results from *in vitro* assay to establish enzyme kinetics, quantitative structure–activity relationship (QSAR, see [Supplementary material](#)) and performed flexible ligand docking to predict plausible binding mode of these derivatives within ChE active sites.

2. Results and discussion

2.1. Chemistry

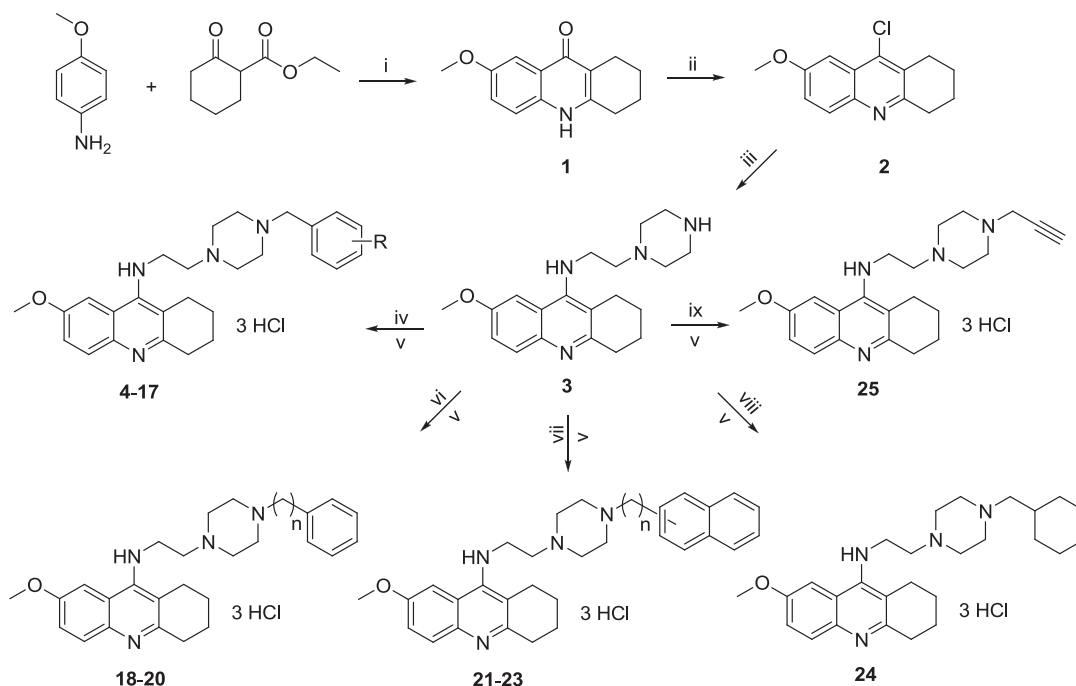
The general synthetic pathway for the novel 7-MEOTA–donepezil like compounds is displayed in [Scheme 1](#). The starting fused ring, 7-methoxy-1,2,3,4-tetrahydroacridin-9(10*H*)-one (**1**), was obtained by the cyclo-condensation reaction of 4-methoxyaniline with ethyl-2-oxocyclohexanecarboxylate using catalytic addition of *p*-toluenesulfonic acid in good yield (74%) [33]. Then, chlorination of **1** into 9-chloro-7-methoxy-1,2,3,4-tetrahydroacridine (**2**) was employed by treatment with phosphoryl chloride, yielding quantitatively. Compound **2** reacted with 1-(2-aminoethyl)piperazine to provide key intermediate 7-methoxy-*N*-(2-(piperazin-1-yl)ethyl)-1,2,3,4-tetrahydroacridin-9-amine (**3**) in good yield (78%). Further step involved alkylation of **3** by differently substituted benzylbromides (derivatives **4–17**), (ω -bromoalkyl)benzenes (**18–20**), 1-/2-(bromomethylnaphthalene) (**21**, **22**), 1-(2-bromoethyl)naphthalene (**23**), (bromomethyl)cyclohexane (**24**) or propargylbromide (**25**) in the presence of *N,N*-diisopropylethylamine (Hunig's base) in CH_2Cl_2 to afford the lead compounds in 65–85% yield. Finally, these compounds were converted into more soluble hydrochloric salts by treatment with hydrochloric gas in methanol.

All synthesized compounds (**3–25**) were sufficiently characterized by the application of the usual combination of ^1H and ^{13}C NMR spectra. The unequivocal assignments were performed by homo- and hetero-correlated two-dimensional NMR experiments (^1H , ^1H -COSY, ^1H , ^{13}C -HSQC, ^1H , ^{13}C -HMBC). Moreover, compound's ESI-MS spectra showing molecular ion $[\text{M}+\text{H}]^+$ peaks and elemental analysis further validated their structure. All spectroscopic measurements confirmed the structure and high purity of the synthesized compounds.

2.2. Evaluation of AChE and BChE inhibition activity

7-MEOTA–donepezil hybrids were evaluated *in vitro* as inhibitors of *Eleutherophorus electricus* AChE (*EeAChE*), human recombinant AChE (*hAChE*), equine serum BChE (*eqBChE*) and human plasmatic BChE (*hBChE*), following Ellman's spectrophotometric method [53]. The inhibitory activities of novel compounds were compared to those of THA, 7-MEOTA and donepezil. All of the novel target analogues proved to be very potent inhibitors of all cholinesterases displaying inhibition abilities mostly in micromolar to sub-micromolar range. Several structure–activity relationships (SAR) are evident from the data in [Table 1](#).

The results of intermediate **3** showed controversial inhibitory activities displaying higher inhibition for *EeAChE* and *eqBChE* than for corresponding enzymes of human origin. Compounds containing electron-withdrawing groups in position 4- of benzyl ring (**8**, **9**, **10**) revealed inhibition potencies in micromolar range and sub-micromolar range for *hAChE* and *EeAChE*, respectively, being almost two- to three-times more selective in inhibiting *hAChE* than *hBChE*. Similarly, the analogues substituted in position 4 of benzyl moiety with electron-donating substituents (**5**, **6**, **11**, **14**) displayed selective profile for inhibition of *hAChE* likewise maintaining enhanced inhibitory activity for *EeAChE*. On the contrary, methylsulfanyl derivative **15** exerted improved inhibition properties for



Scheme 1. Synthesis of 7-MEOTA–donepezil like compounds (**4–25**). Reagents and conditions: (i) *p*-toluenesulfonic acid, toluene, reflux, Dean–Stark trap; diphenylether, 220 °C; (ii) POCl_3 , reflux; (iii) 1-(2-aminoethyl)piperazine, phenol, 120–130 °C; (iv) benzylbromide, Hunig's base, CH_2Cl_2 , reflux; (v) HCl (g), MeOH; (vi) (ω -bromoalkyl)benzene, Hunig's base, CH_2Cl_2 , reflux; (vii) 1-/2-(bromomethylnaphthalene) or 1-(2-bromoethyl)naphthalene, Hunig's base, CH_2Cl_2 , reflux; (viii) (bromomethyl)cyclohexane, Hunig's base, CH_2Cl_2 , reflux; (ix) propargylbromide, Hunig's base, CH_2Cl_2 , reflux.

Table 1Inhibitory activities of *hAChE*, *hBChE*, *EeAChE* and *eqBChE* expressed as IC_{50} values and selectivity for *hAChE*.

Compound	R	<i>n</i>	<i>hAChE</i> $IC_{50} \pm SEM$ (μM) ^a	<i>hBChE</i> $IC_{50} \pm SEM$ (μM) ^a	<i>EeAChE</i> $IC_{50} \pm SEM$ (μM) ^a	<i>eqBChE</i> $IC_{50} \pm SEM$ (μM) ^a	Selectivity for <i>hAChE</i> ^b
3	—	—	11.96 \pm 0.32	211.20 \pm 3.43	0.80 \pm 0.08	2.07 \pm 0.13	17.65
4	—	1	8.88 \pm 2.40	0.73 \pm 0.07	1.10 \pm 0.19	3.08 \pm 0.29	0.08
5	4-Br	1	1.12 \pm 0.11	17.95 \pm 1.51	0.38 \pm 0.07	6.26 \pm 0.60	16.02
6	4-CH ₃	1	3.21 \pm 0.50	4.33 \pm 0.27	0.97 \pm 0.14	3.19 \pm 0.53	1.35
7	3,5-diCH ₃	1	2.38 \pm 0.23	10.02 \pm 2.43	1.07 \pm 0.07	2.46 \pm 0.17	4.21
8	4-NO ₂	1	1.92 \pm 0.44	6.60 \pm 0.62	0.53 \pm 0.10	5.24 \pm 0.47	3.44
9	4-CN	1	5.06 \pm 0.73	7.24 \pm 0.96	0.69 \pm 0.18	5.19 \pm 0.55	1.43
10	4-COOCH ₃	1	3.20 \pm 0.59	7.15 \pm 0.55	0.41 \pm 0.03	2.07 \pm 0.14	2.23
11	4-CF ₃	1	1.16 \pm 0.22	8.79 \pm 1.29	0.69 \pm 0.08	3.35 \pm 0.34	7.58
12	3-CH ₃	1	1.38 \pm 0.15	1.84 \pm 0.17	1.22 \pm 0.18	2.11 \pm 0.19	1.33
13	2-CH ₃	1	3.51 \pm 0.36	0.84 \pm 0.12	2.56 \pm 0.90	5.19 \pm 1.23	0.24
14	4- <i>i</i> Pr	1	3.04 \pm 0.61	3.48 \pm 0.80	2.16 \pm 0.35	2.47 \pm 0.41	1.14
15	4-SCH ₃	1	2.41 \pm 0.39	0.62 \pm 0.18	1.95 \pm 0.14	3.60 \pm 0.45	0.26
16	3-Br	1	1.59 \pm 0.32	0.71 \pm 0.06	0.78 \pm 0.12	2.42 \pm 0.32	0.44
17	2-Br	1	1.40 \pm 0.16	1.94 \pm 0.11	1.27 \pm 0.14	1.72 \pm 0.28	1.39
18	—	2	14.95 \pm 2.85	1.91 \pm 0.37	1.64 \pm 0.34	3.13 \pm 0.42	0.13
19	—	3	2.59 \pm 0.20	2.82 \pm 0.38	1.52 \pm 0.25	1.35 \pm 0.17	1.09
20	—	5	2.77 \pm 0.34	2.25 \pm 0.40	0.94 \pm 0.18	1.68 \pm 0.08	0.81
21	2-naphthyl	1	2.57 \pm 0.12	3.43 \pm 0.32	2.23 \pm 0.17	2.20 \pm 0.30	1.33
22	1-naphthyl	1	1.63 \pm 0.16	8.48 \pm 1.02	0.64 \pm 0.11	3.52 \pm 0.45	5.20
23	1-naphthyl	2	1.94 \pm 0.26	5.46 \pm 0.34	0.33 \pm 0.02	2.11 \pm 0.19	2.81
24	—	—	2.50 \pm 0.33	1.08 \pm 0.09	1.30 \pm 0.09	1.21 \pm 0.15	0.43
25	—	—	12.91 \pm 0.70	0.42 \pm 0.01	1.27 \pm 0.18	4.74 \pm 0.18	0.03
THA	—	—	0.28 \pm 0.01	0.023 \pm 0.003	0.044 \pm 0.011	0.052 \pm 0.003	0.08
7-MEOTA	—	—	10.50 \pm 2.00	21.00 \pm 3.00	0.41 \pm 0.05	0.40 \pm 0.02	2.00
Donepezil	—	—	0.021 \pm 0.0023 ^c	7.27 \pm 0.62 ^c	—	—	340.0

^a Results are expressed as the mean of at least three experiments.^b Selectivity for *hAChE* is determined as ratio *hBChE* IC_{50} /*hAChE* IC_{50} .^c Data taken from Ref. [41].

hBChE over *hAChE*, however, this trend was not observed among enzymes of animal source.

Considering alkyl containing benzyl derivatives (**6**, **7**, **12**, **13**, **14**), the effect of position to *hAChE* inhibitory ability could be elucidated as follows: i) the most active derivative for *hAChE* inhibition was compound **12** bearing methyl in position 3-; ii) introduction of second methyl group into position 5- (**7**) decreased *hAChE* inhibitory ability almost two-times; iii) substitution by methyl in position 2- (**13**) was the least tolerated for *hAChE* as well as for *EeAChE* inhibition, such peculiarity could be elucidated by the steric hindrance of methyl group hampering ligand free rotation in term of accommodation into the enzyme active site; iv) derivative with alkyl chains in position 4- (**6**, **14**) expressed very close inhibition properties presuming that branching and bulkiness of alkyl has negligible effect for *hAChE* inhibition ability. Regarding *hBChE* inhibitory potencies for the same subset of compounds, derivative **13** demonstrated the best inhibition properties proposing that other positions for substitution, branching or di-substitution are not convenient for *hBChE* inhibition.

Except for analogue **12** that showed similar inhibition potency as **16**, bromo-substituted benzyl derivatives (**5**, **16**, **17**) turned out to be two- to three times more potent *hAChE* inhibitors than their methylated counterparts, highlighting analogue **5**. Similar observations can be made for *EeAChE* inhibition. Noteworthy, compound **5** showed the best selective profile for *hAChE* in the whole 7-MEOTA–donepezil series.

Taking into account the length of the linker between phenyl and piperazine moieties (**4**, **18**, **19**, **20**), inhibition potency for *hAChE* increases to three methylene units (**19**), further elongation slightly decreases the potency. Furthermore, the activity for *EeAChE* goes up to five methylenes (**20**). The optimal linker for *hBChE* inhibition was one methylene unit (**4**), further elongation led to activity decrement. Inconsistent data were obtained for *eqBChE*, where the most active derivative comprised three methylene tether, shortening or elongation decreased the potency.

Substitution with naphthyl (**21**, **22**, **23**) provided derivatives preferentially inhibiting AChE over BChE enzymes. However, no further SAR can be established due to a small subset.

The majority of tested hybrids did not show a clear selectivity, although there were some exceptions. Very interesting inhibition profile was exerted by aliphatic derivatives (**24** and **25**). Both of them showed substantial selectivity towards *hBChE* highlighting **24** as the most potent *hBChE* inhibitor in the series with improved selectivity profile over *hAChE*, however, still being one order of magnitude worse inhibitor compared to THA.

Comparing to the previously published data, Omran et al. made large observation for sixty-four new indanones and thiaindanones linked with differently substituted benzylpiperazines [34]. The oxime derivative bearing 2-fluorobenzylpiperazine fragment (**26**, Fig. 2) with IC_{50} value 0.06 μM against *EeAChE* had the inhibitory potency approaching to that of donepezil. Unfortunately, 7-MEOTA–donepezil hybrids revealed as one or two orders less potent inhibitors of *EeAChE*. Ismail's group investigated a series of thiophene, isatine and oxindole derivatives related to donepezil [35,36]. Inhibition properties against AChE were assayed *in vivo* using male albino Wistar rats (oral administration of compounds at concentration equivalent to donepezil). Obtained results for some analogues displayed inhibitory activities better than that found for donepezil suggesting that the most potent derivative **27** (Fig. 2) inhibited AChE up-to 55%. Not surprisingly, propargylamine group was shown to be an important feature for derivatives to exhibit both AChE and BChE inhibitory activities. From this point of view, compound **ASS234** (Fig. 2) conceived by a conjunctive approach that combines *N*-benzylpiperidine motif of donepezil and *N*-(5-benzoyloxy-1-methyl-1*H*-indol-2-yl)methyl-*N*-methylprop-2-yn-1-amine of **PF9601N** (*N*-(2-propynyl)-2-(5-benzoyloxy-indolyl)methylamine) was reported as potent *EeAChE*, *eqBChE*, MAO-A and MAO-B inhibitor [37,38]. Based on the results from current study, 7-MEOTA–donepezil like hybrid **25** showed potency only one order of magnitude less against *EeAChE* and *eqBChE*. The Camps group

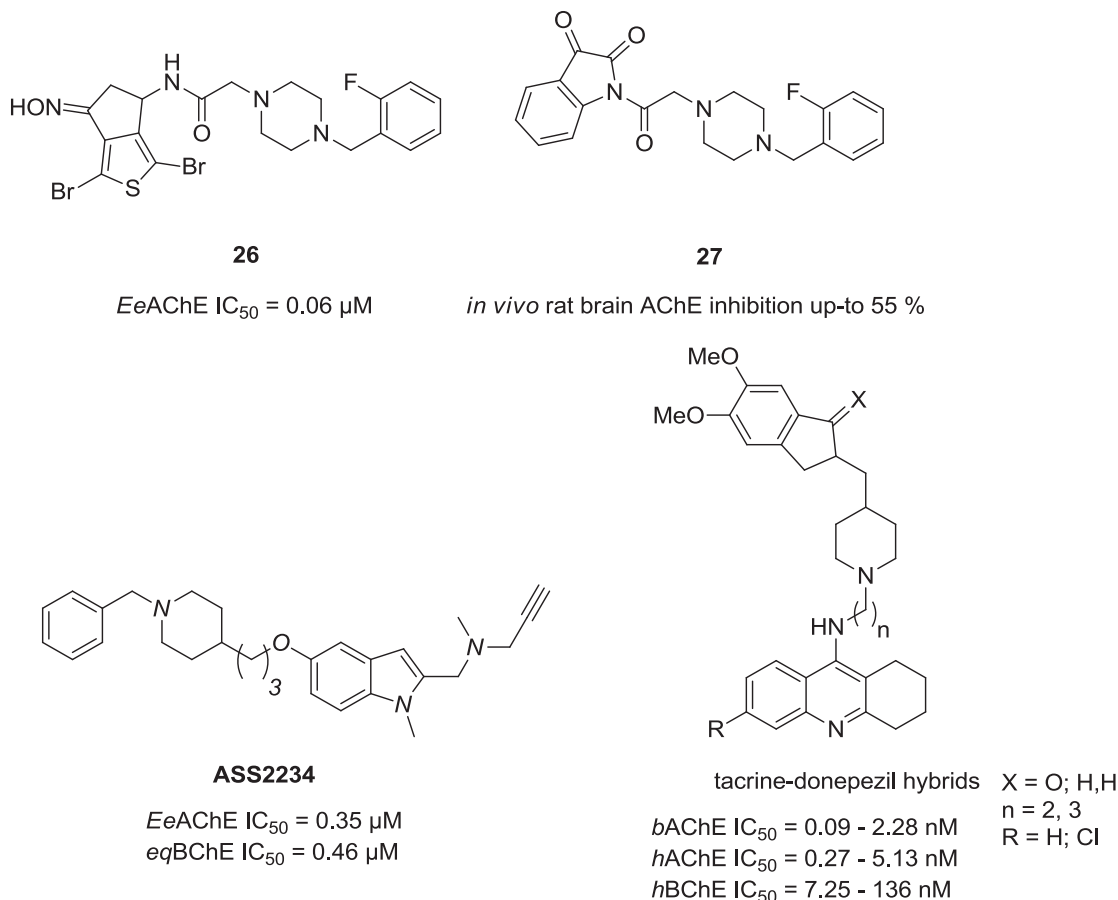


Fig. 2. Previously published donepezil-related compounds with anti-cholinesterase properties.

obtained a new series of heterodimers by linking a THA pharmacophore with indan or indanone core from donepezil by piperidine linkage [39,40]. As reported, such combination provided nanomolar to picomolar inhibition of bovine AChE (*bAChE* IC₅₀ = 0.09–2.28 nM) and *hAChE* (IC₅₀ = 0.27–5.13 nM), while being slightly less potent against *hBChE* (IC₅₀ = 7.25–136 nM). Structural motif of these inhibitors is depicted in Fig. 2.

Overall, none of the tested compounds in the 7-MEOTA–donepezil series exceeded *hAChE* inhibition activities of donepezil and THA. Considering donepezil *hBChE* inhibition, comparable or even better activities were obtained. Almost all of the novel 7-MEOTA–donepezil hybrids revealed better *hAChE*/*hBChE* inhibition profile than parent compound 7-MEOTA. On the basis of the IC₅₀ values, analogues **5**, **11**, **23** and **25** proved to be interesting compounds in the 7-MEOTA–donepezil subset.

2.3. Kinetic study of ChE inhibition

Enzyme kinetic analysis of 7-MEOTA–donepezil hybrids, estimation of *K_i* and analysis of type of inhibition were performed with crude extract of AChE prepared from rat brain presuming the high degree of amino acid residues homology in the active site with other AChE family enzymes. Values of *K_i* are given at Table 2. Statistical comparison with 7-MEOTA showed significantly higher values of *K_i* for all tested analogs, indicating some loss of inhibition in comparison with the parent compound. Analyses by Cornish–Bowden transformation (*S/V_i* vs. inhibitor concentrations, Fig. 3 showing illustrative result for compound **4**) were used for definitive identification of the type of inhibition [42]. *K_i* calculations were derived from Dixon plot (Fig. 4) [43]. For all the tested

compounds, lines intercepted below y axis indicated mixed type inhibition. This mode of inhibition points to an inhibitors with dual-binding site character. Such character assumes binding of the inhibitor in the CAS as well as in the PAS of AChE.

2.4. Molecular modeling studies

The affinity of the compounds under the study toward *hAChE* (human recombinant AChE, PDB ID: 4EY7) [16], *hBChE* (human BChE, PDB ID: 4BDS) [44] and *EeAChE* (electric eel AChE, PDB ID: 1C2O) [45] enzymes was also investigated by flexible molecular docking in AutoDock Vina 1.1.2 (for the details the reader is kindly referred to the methodological part) [46]. Results of molecular modeling studies for *hBChE* and *EeAChE* can be found in Supplementary material. Molecular models of these cholinesterase homologs, except from *eqBChE* which was unavailable, were obtained from the PDB database. All 23 ligands were modeled and docked in a protonated form following the results of microspecies

Table 2
K_i values for selected 7-MEOTA–donepezil like compounds.

Compound	<i>K_i</i> ^a	SD
4	9.69E-06	2.14E-06
7	1.05E-05	1.94E-06
12	6.52E-06	1.09E-06
18	8.79E-06	5.75E-07
15	9.89E-06	2.40E-06
16	3.88E-06	5.41E-07
25	5.10E-06	3.55E-06
7-MEOTA	2.29E-06	5.94E-07

^a Results are expressed as the mean ± SD of at least six experiments.

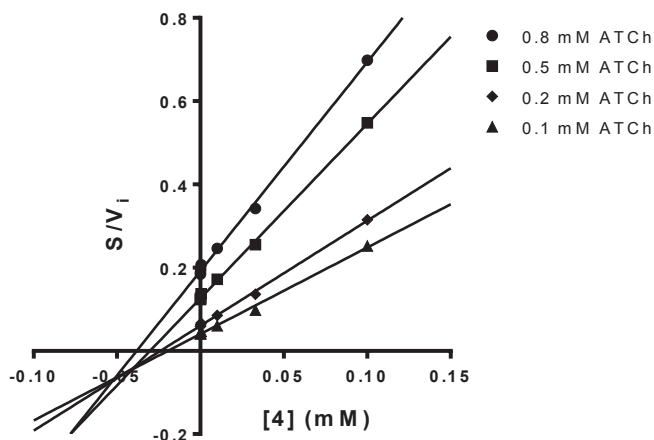


Fig. 3. Cornish–Bowden plot for the inhibition of compound **4** on the hydrolysis activity of AChE. Concentrations of the substrate (acetylthiocholine; ATCh) were 0.1; 0.2; 0.5 and 0.8 mM; concentrations of **4** ranged between 0.33 and 100 μ M.

distribution analysis at pH = 7.4 by MarvinSketch 6.2.0 program [47]. As a compromise, each ligand was protonated on the tetrahydroacridine and the distal piperazine nitrogen atom to represent the calculated predominant ionization. Since the results of molecular docking considerably depend on the extension of the flexible enzyme part, a spherical selection of $R = 11$ Å centered approximately in the middle of the enzyme active site to select flexible residues was used. By this approach 34–40 residues were chosen in the enzyme models (for details see the Experimental section about Molecular modeling studies) to ensure proper settling of the ligands in the active sites. All these residues delineate the enzyme gorge shape enabling its motion and/or enlargement to some extent.

With respect to the results of the IC_{50} survey, the top scoring docked poses of inhibitors (**5** for hAChE; [Supplementary material](#) provides results for docking studies for **25** in hBChE, **23** in EeAChE) exhibiting highest activity in biochemical experiments were minutely explored. In the **5**-hAChE complex ([Fig. 5](#)) the THA moiety is stacked by π – π interaction to Trp286 (3.5 Å) and Tyr124 (3.8 Å) in the PAS. Further stabilization of the complex is reached by another π – π interaction of 4-bromophenyl aromatic ring of the ligand to Trp86 (3.7 Å) in the CAS. The spacer connecting the tacrine

moiety to the distal aromatic ring is aligned along the gorge being surrounded by Tyr341 and His447 residues. However, the distance between the spacer and the residues resulted in this case is mostly longer than demarcated to support the mutual affinity by non-covalent interactions. For instance, the length of the hydrogen bond between the hydroxyl function of Tyr341 and the non-protonated nitrogen atom of the ligand piperidine moiety is 4.3 Å, which somewhat exceeds the 3.5 Å limit for this type of weak interaction [48]. All these interactions, beside those not reflected here, contribute more or less to estimated binding energy of the **5**-hAChE complex (–13.8 kcal/mol) and give a justification of the high IC_{50} observed.

If seen from a qualitative point of view, the presented molecular docking study conforms to widely accepted conditions for non-covalent interactions of dual-binding ligands with cholinesterase homologs. Referring to the literature it is well known that compounds bearing the THA moiety may interact with aromatic amino acid residues in the proximity of CAS [5052]. However, in the case of **5**-hAChE the THA moiety was found to interact with Trp286 and Tyr124 in the PAS, occupying the entrance of the active site. Due to this blockage of the enzyme straight in its mouth, such a reversed tacrine orientation may have a positive influence on increasing the ligand inhibition activity. As for the **25**-hAChE and **5**-EeAChE ([Supplementary material](#)) complexes, the THA moiety was stabilized by a usual π – π interaction with Trp82 and Trp86, respectively, in the CAS. Another intensifying of the binding modes was brought about by cation– π interactions, hydrogen bonds and hydrophobic contacts.

Unfortunately, statistical analysis of correlation between the calculated binding energies and $\log(IC_{50})$ proved no significant dependence. Resulting low Pearson's correlation coefficients ($r = 0.08$ – 0.42) indicate that simplifications and generalizations involved in the molecular docking procedure performed within the study are still very rough to satisfactorily fit the experimental data. But regarding this disappointing result, it is also necessary to bear in mind that biological experiments are in the essence too complicated to be reproduced as such by current *in silico* methods.

3. Conclusion

The present study reports the synthesis and biological evaluation of a subset of novel dual binding site 7-MEOTA–donepezil like derivatives. Our results showed that synthesized compounds had cholinesterase inhibitory activity with IC_{50} values ranging in micromolar to sub-micromolar scale against enzymes of human (hAChE, hBChE) as well as of animal origin (EeAChE, eqBChE). Analogues **5**, **11**, **23** and **25** were pointed as the most active. Based on the kinetic analysis together with molecular modeling studies, we can infer that several new hybrids have targeted both the CAS and the PAS of AChE. The QSAR models provided the necessary background how to find more selective as well as more potent inhibitors of cholinesterases (for QSAR studies see [Supplementary material](#)). The new derivatives showed a rather moderate degree of potency against the enzymes, but the molecular skeleton allows for structural modifications that are presently under study to explore the potential of the series toward new cholinergic agents useful in the treatment of AD.

4. Experimental section

4.1. Chemistry

Analytical grade reagents were purchased from Sigma–Aldrich, Merck and Fluka and were used as supplied. Reactions were monitored via thin layer chromatography (TLC) using precoated

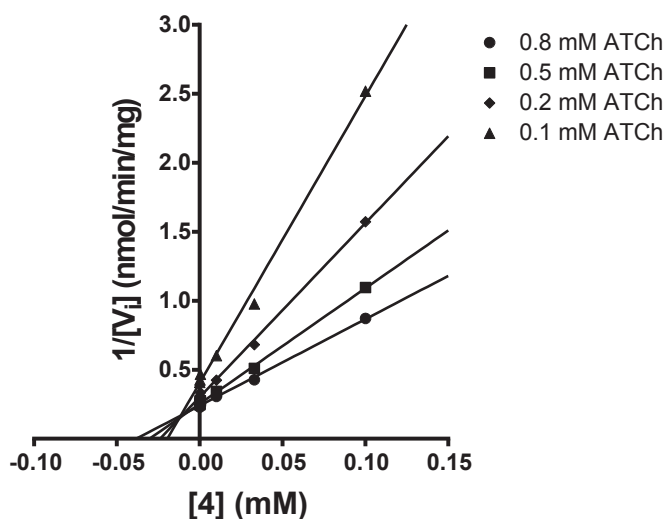


Fig. 4. Dixon plot for the inhibition of compound **4** (0.33 μ M–0.1 mM) on the hydrolysis activity of AChE in the presence of different substrate concentrations (ATCh; 0.1–0.8 mM).

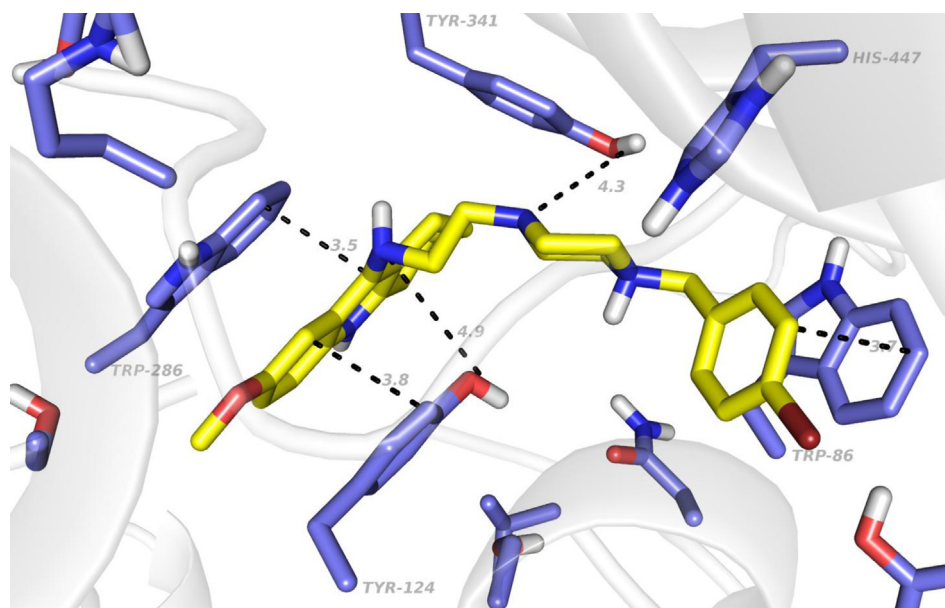


Fig. 5. Top scoring binding mode of **5** in the active site of hAChE (PDB ID: 4EY7) with the binding energy estimate -13.8 kcal/mol. The ligand is colored in yellow, the flexible residues are shown in blue. For the sake of better clarity the majority of the flexible residues is not displayed. The figure was created with PyMol viewer [49]. (For interpretation of the references to color in this figure legend, the reader is referred to the web version of this article.)

silica gel 60 F₂₅₄ TLC aluminum sheet. Column chromatography was performed with silica gel 0.063–0.200 mm.

All compounds were fully characterized by melting points (mp), NMR spectra, elemental analysis and mass spectrometry. Melting points were determined on a microheating stage PHMK 05 (VEB Kombinat Nagema, Radebeul, Germany) and are uncorrected. Elemental analysis (C, H, N) were performed by Mrs. Venceslava Hronova (Department of Pharmaceutical Chemistry and Drug Control, Faculty of Pharmacy in Hradec Kralove) on an automatic microanalyser CHNS–O CE instrument (FISON EA 1110, Italy). NMR spectra were recorded on a Varian VNMR S500 (operating at 500 MHz for ¹H and 125 MHz for ¹³C; Varian Comp. Palo Alto, USA). The chemical shifts (δ) are given in ppm, related to tetramethylsilane (TMS) as an internal standard. The coupling constants (J) are reported in Hz. Splitting patterns are designed as s, singlet; d, doublet; dd, doublet of doublets t, triplet; m, multiplet. Mass spectra were recorded using combination of high performance liquid chromatography (HPLC) and mass spectrometry. HP1100 HPLC system was obtained from Agilent Technologies (Waldbronn, Germany). It consisted of vacuum degasser G1322A, quaternary pump G1311A, autosampler G1313A and quadrupole mass spectrometer MSD1456 VL equipped with electrospray ionization (ESI) source. Nitrogen for mass spectrometer was supplied by Whatman 75-720 nitrogen generator. Data were collected in positive ion mode with an ESI probe voltage of 4000 V. The pressure of nebulizer gas was set up to 35 psig. Drying gas temperature was operated at 335 °C and flow at 13 L/min.

4.1.1. Synthesis of intermediate 7-methoxy-1,2,3,4-tetrahydroacridin-9(10H)-one (**1**)

A mixture of 4-methoxyaniline (12.3 g, 0.1 mol) and ethyl 2-oxocyclohexancarboxylate (18.7 g, 0.11 mol) and *p*-toluenesulfonic acid monohydrate (0.3 g) in toluene (300 mL) was stirred and refluxed for 8 h with a Dean–Stark trap to remove water. Evaporation of the toluene gave the crude enaminoester which was dissolved in warm diphenylether (80 mL). The flask was fitted with a Dean–Stark trap to remove ethanol and the mixture was heated

at 220 °C and maintained until the starting material had disappeared (approximately 30 min, controlled by TLC with ethyl acetate/methanol 95:5 v/v as eluent). The mixture was allowed to cool to room temperature and hexane (200 mL) was added. The precipitated solid was collected by filtration and washed with additional hexane (200 mL) with no further purification to give **1** (17.0 g, 74%) as yellow solid: mp > 300 °C [33]; ¹H NMR (CDCl₃) δ 1.73 (m, 4H, 2 \times CH₂, H-2,3), 2.43 (t, 2H, CH₂, H-1, J = 6.0 Hz), 2.70 (t, 2H, CH₂, H-4, J = 6.0 Hz), 3.95 (s, 3H, OCH₃), 7.30 (dd, 1H, CH, H-6, J = 9.2, 2.8 Hz), 7.38 (d, 1H, CH, H-8, J = 2.4 Hz), 7.86 (d, 1H, CH, H-5, J = 9.2 Hz); ¹³C NMR (CDCl₃) δ 21.7 (C-3), 22.0 (C-1), 22.2 (C-2), 27.3 (C-4), 55.5 (OCH₃), 101.4 (C-8), 122.0 (C-6), 126.2 (C-8a), 128.9 (C-9a), 130.2 (C-5), 142.7 (C-10a), 156.6 (C-7), 158.0 (C-4a), 175.4 (C=O); ESI-MS: m/z 230.0 [M]⁺ (calculated for: [C₁₄H₁₆NO₂]⁺ 230.1); Anal. Calcd for C₁₄H₁₅NO₂: C, 73.34; H, 6.59; N, 6.11. Found: C, 73.28; H, 6.80; N, 6.02.

4.1.2. 9-Chloro-7-methoxy-1,2,3,4-tetrahydroacridine (**2**)

7-Methoxy-1,2,3,4-tetrahydroacridin-9(10H)-one (**1**) (10.0 g, 4.3 mmol) was dissolved in phosphoryl chloride (34.8 g, 22.4 mmol) with good stirring (exothermic reaction occurred). After refluxing for 1 h, the reaction mixture was cooled and excessive phosphoryl chloride was removed with distillation under the normal pressure. The residue was dissolved in CH₂Cl₂ (50 mL) and alkalinized with 25% ammonium hydroxide with addition of ice (300 g). The organic layer was washed with water, dried over CaCl₂ and the solvent was evaporated. The crude product was purified by the flash chromatography on triethylammonium saturated silica gel (CH₂Cl₂/EtOAc, 9:1) to give **2** (10.8 g, 100%) as yellow solid: mp > 121.8–123.5 °C [33]; ¹H NMR (CDCl₃) δ 1.93 (m, 4H, 2 \times CH₂, H-2,3), 3.0 (m, 2H, CH₂, H-1), 3.08 (m, 2H, CH₂, H-4), 3.95 (s, 3H, OCH₃), 7.30 (dd, 1H, CH, H-6, J = 9.2, 2.8 Hz), 7.38 (d, 1H, CH, H-8, J = 2.4 Hz), 7.86 (d, 1H, CH, H-5, J = 9.2 Hz). ¹³C NMR (CDCl₃) δ 22.6, 22.7 (C-2,3), 27.6 (C-1), 33.8 (C-4), 55.5 (OCH₃), 101.4 (C-8), 121.9 (C-6), 126.2 (C-8a), 128.9 (C-9a), 130.2 (C-5), 139.9 (C-9), 142.7 (C-10a), 156.6 (C-7), 157.9 (C-4a); ESI-MS: m/z 248.0 [M]⁺ (calculated for: [C₁₄H₁₅ClNO]⁺ 248.1); Anal. Calcd for C₁₄H₁₄ClNO: C, 67.88; H, 5.70; N, 5.65. Found: C, 67.95; H, 5.81; N, 5.42.

4.1.3. 7-Methoxy-N-(2-(piperazin-1-yl)ethyl)-1,2,3,4-tetrahydroacridin-9-amine (3)

Phenol (10.0 g) and **2** (0.5 g, 2.0 mmol) were heated and stirred at 80–90 °C until a homogenous solution was obtained. 1-(2-aminoethyl)piperazine (1.04 g, 8.0 mmol) was added and the temperature of reaction was raised to 120–130 °C and maintained until starting material disappeared (2–4 h). After cooling, the mixture was poured into 20% sodium hydroxide and extracted with CH₂Cl₂. The organic layer was washed with brine and water, dried over sodium sulfate and evaporated to dryness under reduced pressure. The oily residue was purified via flash chromatography EtOAc/MeOH/NH₃ (25% aq.) (6:2:0.2) as eluent to give **3** (0.54 g, 78%) as yellow oil: ¹H NMR (D₂O): δ 7.58 (d, 1H, CH, H-5, *J* = 9.2 Hz), 7.40 (dd, 1H, CH, H-6, *J* = 9.2, 2.4 Hz), 7.31 (s, 1H, CH, H-8), 4.27 (t, 2H, CH₂, H-1', *J* = 6.0 Hz), 3.96 (s, CH₃, OCH₃), 3.78 (m, 4H, 2 × CH₂, H-3', H-6'), 3.62 (m, 6H, 3 × CH₂, H-4', H-5', H-7'), 3.38 (m, 2H, CH₂, H-2'), 2.98 (m, 2H, CH₂, H-4), 2.78 (m, 2H, CH₂, H-1), 1.80 (m, 4H, 2 × CH₂, H-2, H-3); ¹³C NMR (D₂O): δ 157.5 (C-10a), 155.5 (C-9), 151.7 (C-4a), 132.8 (C-7), 124.5 (C-6), 121.2 (C-5), 118.4 (C-8a), 114.2 (C-9a), 103.4 (C-8), 56.9 (OCH₃), 53.9 (C-1'), 49.8 (C-4', C-5'), 48.3 (C-3', C-6'), 41.4 (C-2'), 28.7 (C-4), 25.5 (C-1), 22.2, 20.7 (C-2, C-3); ESI-MS: *m/z* 341.0 [M]⁺ (calculated for: [C₂₀H₂₉N₄O]⁺ 341.2); Anal. Calcd for C₂₀H₂₈N₄O: C, 70.56; H, 8.29; N, 16.46. Found: C, 70.46; H, 8.31; N, 16.30.

4.1.4. General procedure for synthesis of novel 7-MEOTA–donepezil like compounds (4–25)

Intermediate **3** (0.2 g, 0.6 mmol) was dissolved in anhydrous CH₂Cl₂ and Hunig's base (0.45 g, 3.6 mmol) with appropriate alkylbromide (1.8 mmol) was added. The reaction mixture was refluxed under nitrogen atmosphere overnight followed by evaporation of volatile solvents under reduced pressure. The crude product was purified by flash chromatography eluting EtOAc/MeOH/NH₃ (25% aq.) (40:1:0.2–15:1:0.2) to obtain yellow-to-white oily residue. Resulting free bases were dissolved in methanol and gassed with hydrochloride acid to obtain final products as yellow-to-white salts in 65–85% yields.

4.1.4.1. N-[2-(4-benzylpiperazin-1-yl)ethyl]-7-methoxy-1,2,3,4-tetrahydroacridin-9-amine trihydrochloride (4). Yellow solid (0.25 g, 80%); mp = 152.3–154.4 °C; ¹H NMR (CD₃OD): δ 7.96 (d, 1H, CH, H-5, *J* = 9.2 Hz), 7.81 (s, 1H, CH, H-8), 7.65 (m, 2H, 2 × CH, H-10', H-12'), 7.54 (dd, 1H, CH, H-6, *J* = 9.2, 2.3 Hz), 7.44 (m, 3H, 3 × CH, H-9', H-11', H-13'), 4.25 (m, 4H, 2 × CH₂, H-3', H-6'), 3.96 (s, 3H, OCH₃), 3.15 (m, 2H, CH₂, H-7'), 3.04 (m, 6H, 3 × CH₂, H-4, H-4', H-5'), 2.81 (m, 2H, CH₂, H-1), 2.49 (m, 4H, 2 × CH₂, H-1', H-2') 1.80 (m, 4H, 2 × CH₂, H-2, H-3); ¹³C NMR (CD₃OD): δ 157.0 (C-10a), 155.0 (C-9), 150.6 (C-4a), 142.7 (C-8'), 132.6 (C-7), 131.6 (C-10', C-12'), 129.0 (C-9', C-11', C-13'), 124.5 (C-6), 121.0 (C-5), 118.1 (C-8a), 112.4 (C-9a), 103.6 (C-8), 56.6 (OCH₃), 48.8 (C-7'), 45.6 (C-4', C-5'), 41.3 (C-3', C-6'), 40.0 (C-1', C-2'), 28.1 (C-4), 25.3 (C-1), 21.9, 20.4 (C-2, C-3); ESI-MS: *m/z* 431.0 [M]⁺ (calculated for: [C₂₇H₃₅N₄O]⁺ 431.3); Anal. Calcd for C₂₇H₃₇Cl₃N₄O: C, 60.06; H, 6.91; N, 10.38. Found: C, 60.04; H, 7.08; N, 10.41.

4.1.4.2. N-(2-{4-[(4-bromophenyl)methyl]piperazin-1-yl}ethyl)-7-methoxy-1,2,3,4-tetrahydroacridin-9-amine trihydrochloride (5). Yellow solid (0.28 g, 78%); mp = 173.0–175.2 °C; ¹H NMR (CD₃OD): δ 7.99 (d, 1H, CH, H-5, *J* = 9.2 Hz), 7.82 (s, 1H, CH, H-8), 7.64 (m, 4H, 4 × CH, H-9', H-10', H-12', H-13'), 7.52 (dd, 1H, CH, H-6, *J* = 9.2, 2.1 Hz), 4.26 (m, 2H, CH₂, H-7'), 3.96 (s, 3H, OCH₃), 3.88 (m, 8H, 4 × CH₂, H-4', H-5', H-6'), 3.04 (m, 2H, CH₂, H-4), 2.81 (m, 2H, CH₂, H-1), 2.49 (m, 4H, 2 × CH₂, H-1', H-2'), 1.79 (m, 4H, 2 × CH₂, H-2, H-3); ¹³C NMR (CD₃OD): δ 157.0 (C-10a), 154.9 (C-9), 150.6 (C-4a), 141.7 (C-11'), 133.8 (C-9', C-10', C-12', C-13'), 132.6 (C-8'), 131.9 (C-

7), 124.4 (C-6), 121.0 (C-5), 118.1 (C-8a), 112.4 (C-9a), 103.5 (C-8), 56.6 (OCH₃), 41.2 (C-7'), 48.6 (C-3', C-4', C-5', C-6'), 40.2 (C-1', C-2'), 28.1 (C-4), 25.4 (C-1), 22.0, 20.4 (C-2, C-3); ESI-MS: *m/z* 510.0 [M]⁺ (calculated for: [C₂₇H₃₄BrN₄O]⁺ 510.2); Anal. Calcd for C₂₇H₃₆BrCl₃N₄O: C, 52.40; H, 5.86; N, 9.05. Found: C, 52.16; H, 5.90; N, 9.15.

4.1.4.3. 7-Methoxy-N-(2-{4-[(4-methylphenyl)methyl]piperazin-1-yl}ethyl)-1,2,3,4-tetrahydroacridin-9-amine trihydrochloride (6). Yellow solid (0.27 g, 82%); mp = 168.0–171.2 °C; ¹H NMR ((CD₃)₂SO): δ 8.02 (d, 1H, CH, H-5, *J* = 9.2 Hz), 7.83 (s, 1H, CH, H-8), 7.53 (m, 4H, 4 × CH, H-9', H-10', H-12', H-13'), 7.24 (m, 1H, CH, H-6), 4.28 (m, 4H, 2 × CH₂, H-3', H-6'), 3.97 (s, 3H, OCH₃), 3.52 (m, 6H, 3 × CH₂, H-4', H-5', H-7'), 3.05 (m, 2H, CH₂, H-4), 2.82 (m, 2H, CH₂, H-1), 2.50 (m, 4H, 2 × CH₂, H-1', H-2'), 2.31 (s, 3H, CH₃), 1.80 (m, 4H, 2 × CH₂, H-2, H-3); ¹³C NMR ((CD₃)₂SO): δ 157.3 (C-10a), 155.1 (C-9), 150.9 (C-4a), 139.6 (C-11'), 132.6 (C-8'), 132.0 (C-7), 131.6 (C-9', C-13'), 129.8 (C-10', C-12'), 124.7 (C-6), 121.3 (C-5), 118.4 (C-8a), 112.7 (C-9a), 103.8 (C-8), 65.4 (C-7'), 56.6 (OCH₃), 48.8 (C-4', C-5'), 41.4 (C-3', C-6'), 40.5 (C-1', C-2'), 28.4 (C-4), 25.7 (C-1), 22.2 (CH₃), 21.3, 20.7 (C-2, C-3); ESI-MS: *m/z* 445.0 [M]⁺ (calculated for: [C₂₈H₃₇N₄O]⁺ 445.3); Anal. Calcd for C₂₈H₃₉Cl₃N₄O: C, 60.70; H, 7.10; N, 10.11. Found: C, 60.54; H, 7.36; N, 10.08.

4.1.4.4. N-(2-{4-[(3,5-dimethylphenyl)methyl]piperazin-1-yl}ethyl)-7-methoxy-1,2,3,4-tetrahydroacridin-9-amine trihydrochloride (7). Yellow solid (0.23 g, 70%); mp = 157.8–158.9 °C; ¹H NMR (CD₃OD): δ 7.78 (d, 1H, CH, H-5, *J* = 9.2 Hz), 7.74 (m, 1H, CH, H-8), 7.52 (dd, 1H, CH, H-6, *J* = 9.2, 2.2), 7.25 (m, 2H, 2 × CH, H-9', H-13'), 7.16 (s, 1H, CH, H-11'), 4.45 (m, 2H, CH₂, H-7'), 4.40 (m, 4H, 2 × CH₂, H-3', H-6'), 4.04 (s, 3H, OCH₃), 3.75 (m, 8H, 4 × CH₂, H-1', H-2', H-4', H-5'), 3.09 (m, 2H, CH₂, H-4), 2.93 (t, 2H, CH₂, H-1, *J* = 5.2 Hz), 2.36 (s, 6H, 2 × CH₃), 1.97 (m, 4H, 2 × CH₂, H-2, H-3); ¹³C NMR (CD₃OD): δ 159.4 (C-10a), 157.0 (C-9), 152.2 (C-4a), 144.1 (C-7), 140.5 (C-10', C-12'), 134.1 (C-8'), 133.0 (C-9', C-13'), 130.2 (C-11'), 126.2 (C-6), 121.9 (C-5), 119.8 (C-8a), 114.7 (C-9a), 104.0 (C-8), 61.4 (C-7'), 57.9 (C-4', C-5'), 57.2 (OCH₃), 49.5 (C-1', C-2'), 42.4 (C-3', C-6'), 29.4 (C-4), 26.8 (C-1), 23.2, 21.7 (C-2, C-3), 21.2 (2 × CH₃); ESI-MS: *m/z* 459.0 [M]⁺ (calculated for: [C₂₉H₃₉N₄O]⁺ 459.3); Anal. Calcd for C₂₉H₄₁Cl₃N₄O: C, 61.32; H, 7.28; N, 9.86. Found: C, 61.56; H, 7.34; N, 10.00.

4.1.4.5. 7-Methoxy-N-(2-{4-[(4-nitrophenyl)methyl]piperazin-1-yl}ethyl)-1,2,3,4-tetrahydroacridin-9-amine trihydrochloride (8). Yellow solid (0.29 g, 83%); mp = 169.9–171.1 °C; ¹H NMR (CD₃OD): δ 8.17 (d, 1H, CH, H-5, *J* = 9.2 Hz), 8.15 (s, 1H, CH, H-8), 7.90 (m, 2H, 2 × CH, H-9', H-13'), 7.77 (m, 2H, 2 × CH, H-10', H-12'), 7.52 (dd, 1H, CH, H-6, *J* = 9.2, 2.3 Hz), 4.61 (m, 2H, CH₂, H-7'), 4.38 (m, 4H, 2 × CH₂, H-3', H-6'), 4.01 (s, CH₃, OCH₃), 3.74 (m, 4H, 2 × CH₂, H-4', H-5'), 3.30 (m, 4H, 2 × CH₂, H-1', H-2'), 3.04 (t, 2H, CH₂, H-4, *J* = 6.0 Hz), 2.95 (t, 2H, CH₂, H-1, *J* = 5.7 Hz), 1.98 (m, 4H, 2 × CH₂, H-2, H-3); ¹³C NMR (CD₃OD): δ 159.4 (C-10a), 157.1 (C-9), 150.5 (C-4a), 136.6 (C-11'), 133.9 (C-8'), 131.0 (C-9', C-13'), 129.1 (C-10', C-12'), 125.2 (C-6), 125.0 (C-7), 121.9 (C-5), 119.7 (C-8a), 114.7 (C-9a), 104.1 (C-8), 60.0 (C-7'), 57.0 (OCH₃), 50.5 (C-3', C-4', C-5', C-6'), 42.6 (C-1', C-2'), 29.4 (C-4), 26.6 (C-1), 21.7, 21.2 (C-2, C-3); ESI-MS: *m/z* 476.0 [M]⁺ (calculated for: [C₂₇H₃₄N₅O₃]⁺ 476.3); Anal. Calcd for C₂₇H₃₆Cl₃N₅O₃: C, 55.44; H, 6.20; N, 11.97. Found: C, 55.48; H, 6.23; N, 11.80.

4.1.4.6. 4-[(4-{2-[(7-methoxy-1,2,3,4-tetrahydroacridin-9-yl)amino]ethyl]piperazin-1-yl)methyl]benzonitrile trihydrochloride (9). Yellow solid (0.25 g, 75%); mp = 173.4–175.6 °C; ¹H NMR (CD₃OD): δ 7.25 (d, 1H, CH, H-5, *J* = 9.2 Hz), 7.16 (m, 2H, 2 × CH, H-9', H-13'), 7.07 (m, 2H, 2 × CH, H-10', H-12'), 6.98 (s, 1H, CH, H-8), 6.80 (dd, 1H, CH, H-6, *J* = 9.2, 2.4 Hz), 3.70 (s, CH₃, OCH₃), 3.57 (m, 2H, CH₂, H-7'),

2.79 (m, 8H, 4 × CH₂, H-3', H-4', H-5', H-6'), 2.49 (m, 4H, 2 × CH₂, H-1', H-2'), 2.30 (t, 2H, CH₂, H-4, *J* = 6.0 Hz), 2.10 (t, 2H, CH₂, H-1, *J* = 5.8 Hz), 1.80 (m, 4H, 2 × CH₂, H-2, H-3); ¹³C NMR (CD₃OD): δ 158.8 (C-10a), 156.6 (C-9), 151.7 (C-4a), 145.0 (C-8'), 140.2 (C-11'), 133.8 (C-9', C-13'), 133.3 (C-10', C-12'), 125.6 (C-6), 125.0 (C-7), 121.9 (C-5), 119.1 (C-8a), 114.5 (C-9a), 104.5 (C-8), 57.0 (OCH₃), 50.3 (C-7'), 49.8 (C-3', C-4', C-5', C-6'), 42.6 (C-1', C-2'), 29.2 (C-4), 26.2 (C-1), 23.0, 21.5 (C-2, C-3); ESI-MS: *m/z* 456.0 [M]⁺ (calculated for: [C₂₈H₃₄N₅O]⁺ 456.3); Anal. Calcd for C₂₈H₃₆Cl₃N₅O: C, 59.52; H, 6.42; N, 12.40 Found: C, 59.78; H, 6.33; N, 12.50.

4.1.4.7. Methyl 4-[(4-{2-[(7-methoxy-1,2,3,4-tetrahydroacridin-9-yl)amino]ethyl}piperazin-1-yl)methyl]benzoate trihydrochloride (10). White solid (0.29 g, 83%); mp = 157.6–159.1 °C; ¹H NMR ((CD₃)₂SO): δ 8.17 (d, 1H, CH, H-5, *J* = 9.2 Hz), 7.99 (s, 1H, CH, H-8), 7.96 (m, 2H, 2 × CH, H-9', H-13'), 7.80 (m, 2H, 2 × CH, H-10', H-12'), 7.48 (dd, 1H, CH, H-6, *J* = 9.2, 2.4 Hz), 4.43 (m, 2H, CH₂, H-7'), 4.25 (m, 4H, 2 × CH₂, H-3', H-6'), 3.98 (s, CH₃, OCH₃), 3.90 (s, CH₃), 3.45 (m, 4H, 2 × CH₂, H-4', H-5'), 3.04 (m, 2H, CH₂, H-4), 2.81 (m, 2H, CH₂, H-1), 2.48 (m, 4H, 2 × CH₂, H-1', H-2'), 1.88 (m, 4H, 2 × CH₂, H-2, H-3); ¹³C NMR ((CD₃)₂SO): δ 166.0 (C-14'), 157.1 (C-10a), 154.9 (C-9), 150.6 (C-4a), 139.5 (C-7), 132.6 (C-11'), 131.9 (C-8'), 130.6 (C-9', C-13'), 129.6 (C-10', C-12'), 124.4 (C-6), 121.1 (C-5), 118.1 (C-8a), 112.4 (C-9a), 103.6 (C-8), 56.6 (OCH₃), 56.2 (C-7'), 52.5 (CH₃), 48.1 (C-4', C-5'), 41.2 (C-3', C-6'), 40.2 (C-1', C-2'), 28.1 (C-4), 25.4 (C-1), 21.9, 20.4 (C-2, C-3); ESI-MS: *m/z* 489.0 [M]⁺ (calculated for: [C₂₉H₃₇N₄O₃]⁺ 489.3); Anal. Calcd for C₂₉H₃₉Cl₃N₄O₃: C, 58.25; H, 6.57; N, 9.37 Found: C, 58.15; H, 6.49; N, 9.51.

4.1.4.8. 7-Methoxy-N-[2-(4-{4-(trifluoromethyl)phenyl}methyl)piperazin-1-yl]ethyl]-1,2,3,4-tetrahydroacridin-9-amine trihydrochloride (11). Yellow solid (0.24 g, 68%); mp = 176.6–179.8 °C; ¹H NMR ((CD₃)₂SO): δ 8.03 (d, 1H, CH, H-5, *J* = 9.2 Hz), 7.98 (s, 1H, CH, H-8), 7.90 (m, 2H, 2 × CH, H-9', H-13'), 7.81 (m, 2H, 2 × CH, H-10', H-12'), 7.50 (dd, 1H, CH, H-6, *J* = 9.2, 2.4 Hz), 4.46 (m, 2H, CH₂, H-7'), 4.23 (m, 4H, 2 × CH₂, H-3', H-6'), 3.98 (s, CH₃, OCH₃), 3.57 (m, 4H, 2 × CH₂, H-4', H-5'), 3.02 (m, 2H, CH₂, H-4), 2.80 (m, 2H, CH₂, H-1), 2.50 (m, 4H, 2 × CH₂, H-1', H-2'), 1.90 (m, 4H, 2 × CH₂, H-2, H-3); ¹³C NMR ((CD₃)₂SO): δ 157.1 (C-10a), 154.9 (C-9), 150.6 (C-4a), 132.6 (C-8'), 132.4 (C-11'), 129.8 (C-9', C-10', C-12', C-13'), 126.0 (CF₃), 125.8 (C-7), 124.4 (C-6), 121.1 (C-5), 118.1 (C-8a), 112.4 (C-9a), 103.6 (C-8), 57.0 (C-7'), 56.6 (OCH₃), 48.1 (C-3', C-4', C-5', C-6'), 41.2 (C-1', C-2'), 28.1 (C-4), 25.4 (C-1), 22.0, 20.4 (C-2, C-3); ESI-MS: *m/z* 499.0 [M]⁺ (calculated for: [C₂₈H₃₄F₃N₄O]⁺ 499.3); Anal. Calcd for C₂₈H₃₆Cl₃F₃N₄O: C, 55.32; H, 5.97; N, 9.22 Found: C, 55.44; H, 6.13; N, 9.21.

4.1.4.9. 7-Methoxy-N-[2-(4-{(3-methylphenyl)methyl}piperazin-1-yl)ethyl]-1,2,3,4-tetrahydroacridin-9-amine trihydrochloride (12). Yellow solid (0.27 g, 84%); mp = 168.5–171.2 °C; ¹H NMR ((CD₃)₂SO): δ 8.01 (d, 1H, CH, H-5, *J* = 9.2 Hz), 7.83 (s, 1H, CH, H-8), 7.51 (dd, 1H, CH, H-6, *J* = 9.2, 2.4 Hz), 7.48 (s, 1H, CH, H-13'), 7.45 (d, 1H, CH, H-9', *J* = 7.6 Hz), 7.32 (m, 1H, CH, H-11'), 7.24 (d, 1H, CH, H-12'), 4.26 (m, 4H, 2 × CH₂, H-3', H-6'), 3.96 (s, 3H, OCH₃), 3.54 (m, 4H, 2 × CH₂, H-4', H-5'), 3.36 (m, 2H, CH₂, H-7'), 3.05 (t, 2H, CH₂, H-4, *J* = 5.9 Hz), 2.81 (m, 2H, CH₂, H-1), 2.49 (m, 4H, 2 × CH₂, H-1', H-2'), 2.30 (s, 3H, CH₃), 1.79 (m, 4H, 2 × CH₂, H-2, H-3); ¹³C NMR ((CD₃)₂SO): δ 157.0 (C-10a), 154.9 (C-9), 150.6 (C-4a), 138.2 (C-13'), 136.2 (C-7), 132.6 (C-10'), 132.1 (C-8'), 130.3 (C-12'), 128.9 (C-9', C-11'), 124.4 (C-6), 121.1 (C-5), 118.1 (C-8a), 112.4 (C-9a), 103.6 (C-8), 65.1 (C-7'), 56.6 (OCH₃), 48.3 (C-4', C-5'), 41.2 (C-3', C-6'), 40.3 (C-1', C-2'), 28.1 (C-4), 25.4 (C-1), 21.9, 20.4 (C-2, C-3), 21.1 (CH₃); ESI-MS: *m/z* 445.0 [M]⁺ (calculated for: [C₂₈H₃₇N₄O]⁺ 445.3); Anal. Calcd for C₂₈H₃₉Cl₃N₄O: C, 60.70; H, 7.10; N, 10.11 Found: C, 60.66; H, 7.03; N, 10.31.

4.1.4.10. 7-Methoxy-N-[2-(4-{(2-methylphenyl)methyl}piperazin-1-yl)ethyl]-1,2,3,4-tetrahydroacridin-9-amine trihydrochloride (13). Yellow solid (0.24 g, 75%); mp = 169.2–171.1 °C; ¹H NMR ((CD₃)₂SO): δ 8.01 (d, 1H, CH, H-5, *J* = 9.2 Hz), 7.84 (s, 1H, CH, H-8), 7.66 (d, 1H, CH, H-12', *J* = 7.5 Hz), 7.51 (dd, 1H, CH, H-6, *J* = 9.2, 2.2 Hz), 7.32 (m, 1H, CH, H-11'), 7.25 (m, 2H, 2 × CH, H-9', H-10'), 4.42 (m, 2H, CH₂, H-7'), 4.29 (m, 4H, 2 × CH₂, H-3', H-6'), 3.97 (s, 3H, OCH₃), 3.62 (m, 4H, 2 × CH₂, H-4', H-5'), 2.95 (t, 2H, CH₂, H-4, *J* = 5.8 Hz), 2.83 (m, 2H, CH₂, H-1), 2.49 (m, 4H, 2 × CH₂, H-1', H-2'), 2.45 (s, 3H, CH₃), 1.78 (m, 4H, 2 × CH₂, H-2, H-3); ¹³C NMR ((CD₃)₂SO): δ 157.1 (C-10a), 154.9 (C-9), 150.7 (C-4a), 139.0 (C-13'), 132.7 (C-8'), 132.5 (C-12'), 131.1 (C-9'), 129.9 (C-11'), 127.8 (C-7), 126.3 (C-10'), 124.4 (C-6), 121.1 (C-5), 118.2 (C-8a), 112.4 (C-9a), 103.5 (C-8), 56.6 (OCH₃), 56.1 (C-7'), 48.3 (C-4', C-5'), 41.1 (C-3', C-6'), 40.3 (C-1', C-2'), 28.1 (C-4), 25.5 (C-1), 22.0, 20.4 (C-2, C-3), 19.8 (CH₃); ESI-MS: *m/z* 445.0 [M]⁺ (calculated for: [C₂₈H₃₇N₄O]⁺ 445.3); Anal. Calcd for C₂₈H₃₉Cl₃N₄O: C, 60.70; H, 7.10; N, 10.11 Found: C, 60.68; H, 7.23; N, 10.15.

4.1.4.11. 7-Methoxy-N-[2-(4-{4-(propan-2-yl)phenyl}methyl)piperazin-1-yl]ethyl]-1,2,3,4-tetrahydroacridin-9-amine trihydrochloride (14). Yellow solid (0.29 g, 85%); mp = 173.4–174.9 °C; ¹H NMR ((CD₃)₂SO): δ 8.01 (d, 1H, CH, H-5, *J* = 9.2 Hz), 7.83 (s, 1H, CH, H-8), 7.58 (d, 2H, 2 × CH, H-9', H-13', *J* = 7.9 Hz), 7.52 (dd, 1H, CH, H-6, *J* = 9.2, 2.2 Hz), 7.30 (d, 2H, 2 × CH, H-10', H-12', *J* = 8.0 Hz), 4.37 (m, 2H, CH₂, H-7'), 4.27 (m, 4H, 2 × CH₂, H-3', H-6'), 3.96 (s, 3H, OCH₃), 3.50 (m, 4H, 2 × CH₂, H-4', H-5'), 3.05 (t, 2H, CH₂, H-4, *J* = 6.0 Hz), 2.90 (m, 1H, CH, H-14'), 2.82 (m, 2H, CH₂, H-1), 2.49 (m, 4H, 2 × CH₂, H-1', H-2'), 1.79 (m, 4H, 2 × CH₂, H-2, H-3), 1.19 (s, 6H, 2 × CH₃); ¹³C NMR ((CD₃)₂SO): δ 157.1 (C-10a), 154.8 (C-9), 150.0 (C-4a), 138.1 (C-7), 132.6 (C-11'), 131.6 (C-8'), 126.9 (C-9', C-10', C-12', C-13'), 124.4 (C-6), 121.1 (C-5), 118.2 (C-8a), 112.4 (C-9a), 103.5 (C-8), 58.4 (C-7'), 56.6 (OCH₃), 48.7 (C-4', C-5'), 41.1 (C-3', C-6'), 40.2 (C-1', C-2'), 33.4 (C-14'), 28.1 (C-4), 25.5 (C-1), 23.9 (2 × CH₃), 22.0, 20.4 (C-2, C-3); ESI-MS: *m/z* 473.0 [M]⁺ (calculated for: [C₃₀H₄₁N₄O]⁺ 473.3); Anal. Calcd for C₃₀H₄₃Cl₃N₄O: C, 61.91; H, 7.45; N, 9.63 Found: C, 61.67; H, 7.55; N, 9.81.

4.1.4.12. 7-Methoxy-N-[2-(4-{4-(methylsulfonyl)phenyl}methyl)piperazin-1-yl]ethyl]-1,2,3,4-tetrahydroacridin-9-amine trihydrochloride (15). Yellow solid (0.27 g, 77%); mp = 167.2–170.4 °C; ¹H NMR ((CD₃)₂SO): δ 8.01 (d, 1H, CH, H-5, *J* = 9.2 Hz), 7.83 (s, 1H, CH, H-8), 7.60 (d, 2H, 2 × CH, H-9', H-13', *J* = 8.0 Hz), 7.52 (dd, 1H, CH, H-6, *J* = 9.2, 2.0 Hz), 7.30 (d, 2H, 2 × CH, H-10', H-12', *J* = 8.2 Hz), 4.37 (m, 2H, CH₂, H-7'), 4.27 (m, 4H, 2 × CH₂, H-3', H-6'), 3.97 (s, 3H, OCH₃), 3.50 (m, 4H, 2 × CH₂, H-4', H-5'), 3.05 (t, 2H, CH₂, H-4, *J* = 5.8 Hz), 2.82 (m, 2H, CH₂, H-1), 2.50 (m, 4H, 2 × CH₂, H-1', H-2'), 2.48 (s, 3H, CH₃), 1.79 (m, 4H, 2 × CH₂, H-2, H-3); ¹³C NMR ((CD₃)₂SO): δ 157.0 (C-10a), 154.9 (C-9), 150.6 (C-4a), 144.1 (C-7), 140.5 (C-11'), 132.6 (C-9', C-13'), 132.2 (C-8'), 125.8 (C-10', C-12'), 124.4 (C-6), 121.0 (C-5), 118.1 (C-8a), 112.4 (C-9a), 103.5 (C-8), 61.4 (C-7'), 56.6 (OCH₃), 48.4 (C-4', C-5'), 41.2 (C-3', C-6'), 40.2 (C-1', C-2'), 28.1 (C-4), 25.4 (C-1), 21.9, 20.4 (C-2, C-3), 14.4 (SCH₃); ESI-MS: *m/z* 477.0 [M]⁺ (calculated for: [C₂₈H₃₇N₄O]⁺ 477.3); Anal. Calcd for C₂₈H₃₉Cl₃N₄O₂S: C, 57.38; H, 6.71; N, 9.56; S, 5.47 Found: C, 57.57; H, 6.83; N, 9.45; S, 5.53.

4.1.4.13. N-[2-(4-{(3-bromophenyl)methyl}piperazin-1-yl)ethyl]-7-methoxy-1,2,3,4-tetrahydroacridin-9-amine trihydrochloride (16). Yellow solid (0.30 g, 83%); mp = 196.2–197.5 °C; ¹H NMR (D₂O): δ 7.66 (m, 2H, 2 × CH, H-9', H-10'), 7.53 (d, 1H, CH, H-5, *J* = 9.2 Hz), 7.47 (m, 1H, CH, H-6), 7.40 (m, 2H, 2 × CH, H-11', H-13'), 7.28 (s, 1H, CH, H-8), 4.44 (m, 2H, CH₂, H-7'), 4.22 (m, 4H, 2 × CH₂, H-3', H-6'), 3.93 (s, 3H, OCH₃), 3.62 (m, 4H, 2 × CH₂, H-4', H-5'), 2.95 (m, 2H, CH₂, H-4), 2.69 (m, 2H, CH₂, H-1), 2.50 (m, 4H, 2 × CH₂, H-1', H-2'),

1.89 (m, 4H, 2 × CH₂, H-2, H-3); ¹³C NMR (D₂O): δ 157.3 (C-10a), 155.6 (C-9), 151.4 (C-4a), 134.5 (C-12'), 134.2 (C-8'), 132.9 (C-9', C-10'), 130.7 (C-11', C-13'), 130.2 (C-7), 124.5 (C-6), 121.2 (C-5), 118.2 (C-8a), 114.0 (C-9a), 103.7 (C-8), 60.1 (C-7'), 56.8 (OCH₃), 56.7 (C-1v, C-2'), 49.3 (C-4', C-5'), 42.0 (C-3', C-6'), 28.6 (C-4), 25.2 (C-1), 22.2, 20.7 (C-2, C-3); ESI-MS: *m/z* 510.0 [M]⁺ (calculated for: [C₂₇H₃₃BrN₄O]⁺ 510.2); Anal. Calcd for C₂₇H₃₆BrCl₃N₄O: C, 52.40; H, 5.86; N, 9.05 Found: C, 52.63; H, 5.99; N, 9.15.

4.1.4.14. N-(2-{4-[(2-bromophenyl)methyl]piperazin-1-yl}ethyl)-7-methoxy-1,2,3,4-tetrahydroacridin-9-amine trihydrochloride (17). Yellow solid (0.24 g, 65%); mp = 187.5–189.8 °C; ¹H NMR (D₂O): δ 7.79 (d, 1H, CH, H-5, *J* = 9.2 Hz), 7.60 (dd, 1H, CH, H-6, *J* = 9.2, 2.4 Hz), 7.54 (s, 1H, CH, H-8), 7.40 (m, 8H, 4 × CH, H-9', H-10', H-11', H-12'), 4.61 (m, 2H, CH₂, H-7'), 4.23 (m, 4H, 2 × CH₂, H-3', H-6'), 3.96 (s, CH₃, OCH₃), 3.70 (m, 4H, 2 × CH₂, H-4', H-5'), 2.99 (m, 2H, CH₂, H-4), 2.78 (m, 2H, CH₂, H-1), 2.20 (m, 4H, 2 × CH₂, H-1', H-2'), 1.93 (m, 4H, 2 × CH₂, H-2, H-3); ¹³C NMR (D₂O): δ 157.5 (C-10a), 155.8 (C-9), 151.7 (C-4a), 141.5 (C-13'), 134.5 (C-9', C-10', C-11', C-12'), 133.3 (C-8'), 126.5 (C-7), 124.6 (C-6), 121.4 (C-5), 118.4 (C-8a), 114.3 (C-9a), 103.8 (C-8), 60.6 (C-7'), 56.9 (OCH₃), 49.9 (C-3', C-4', C-5', C-6'), 41.9 (C-1', C-2'), 28.7 (C-4), 25.4 (C-1), 22.3, 20.8 (C-2, C-3); ESI-MS: *m/z* 510.0 [M]⁺ (calculated for: [C₂₇H₃₃BrN₄O]⁺ 510.2); Anal. Calcd for C₂₇H₃₆BrCl₃N₄O: C, 52.40; H, 5.86; N, 9.05 Found: C, 52.39; H, 5.79; N, 8.99.

4.1.4.15. 7-Methoxy-N-{2-[4-(2-phenylethyl)piperazin-1-yl]ethyl}-1,2,3,4-tetrahydroacridin-9-amine trihydrochloride (18). Yellow solid (0.22 g, 68%); mp = 158.4–161.8 °C; ¹H NMR ((CD₃)₂SO): δ 8.01 (d, 1H, CH, H-5, *J* = 9.2 Hz), 7.88 (s, 1H, CH, H-8), 7.54 (dd, 1H, CH, H-6, *J* = 9.2, 2.3 Hz), 7.29 (m, 5H, 5 × CH, H-10', H-11', H-12', H-13', H-14'), 4.29 (m, 4H, 2 × CH₂, H-3', H-6'), 3.98 (s, 3H, OCH₃), 3.54 (m, 4H, 2 × CH₂, H-7', H-8'), 3.10 (m, 4H, 2 × CH₂, H-4', H-5'), 3.06 (m, 2H, CH₂, H-4), 2.83 (m, 2H, CH₂, H-1), 2.49 (m, 4H, 2 × CH₂, H-1', H-2'), 1.81 (m, 4H, 2 × CH₂, H-2, H-3); ¹³C NMR ((CD₃)₂SO): δ 157.1 (C-10a), 155.0 (C-9), 150.6 (C-4a), 137.0 (C-9'), 132.6 (C-7), 128.8 (C-10', C-11', C-12', C-13', C-14'), 124.5 (C-6), 121.1 (C-5), 118.1 (C-8a), 112.4 (C-9a), 103.6 (C-8), 56.5 (OCH₃), 55.7 (C-7', C-8'), 41.1 (C-2', C-6'), 40.2 (C-1', C-2'), 29.5 (C-4', C-5'), 28.1 (C-4), 25.3 (C-1), 22.0, 20.4 (C-2, C-3); ESI-MS: *m/z* 445.0 [M]⁺ (calculated for: [C₂₈H₃₇N₄O]⁺ 445.3); Anal. Calcd for C₂₈H₃₉Cl₃N₄O: C, 60.70; H, 7.10; N, 10.11 Found: C, 60.72; H, 7.03; N, 9.98.

4.1.4.16. 7-Methoxy-N-{2-[4-(3-phenylpropyl)piperazin-1-yl]ethyl}-1,2,3,4-tetrahydroacridin-9-amine trihydrochloride (19). Yellow solid (0.23 g, 69%); mp = 135.4–138.8 °C; ¹H NMR (CD₃OD): δ 7.76 (d, 1H, CH, H-5, *J* = 9.2 Hz), 7.73 (m, 1H, CH, H-8), 7.51 (dd, 1H, CH, H-6, *J* = 9.2, 2.4 Hz), 7.27 (m, 5H, 5 × CH, H-11', H-12', H-13', H-14', H-15'), 4.38 (m, 2H, CH₂, H-7'), 4.02 (s, 3H, OCH₃), 3.73 (m, 4H, 2 × CH₂, H-4', H-5'), 3.30 (m, 8H, 4 × CH₂, H-1', H-2', H-3', H-6'), 3.07 (t, 2H, CH₂, H-4, *J* = 6.1 Hz), 2.91 (t, 2H, CH₂, H-1, *J* = 5.7 Hz), 2.74 (t, 2H, CH₂, H-9', *J* = 7.6), 2.15 (m, 2H, CH₂, H-8'), 1.95 (m, 4H, 2 × CH₂, H-2, H-3); ¹³C NMR (CD₃OD): δ 159.4 (C-10a), 157.0 (C-9), 152.2 (C-4a), 141.3 (C-10'), 134.1 (C-7), 129.7 (C-12', C-14'), 129.5 (C-11', C-15'), 127.5 (C-13'), 126.2 (C-6), 121.9 (C-5), 119.8 (C-8a), 114.7 (C-9a), 104.0 (C-8), 57.9 (C-2'), 57.5 (C-4', C-5'), 57.2 (OCH₃), 50.4 (C-1'), 49.8 (C-3', C-6'), 42.4 (C-7'), 33.4 (C-9'), 29.4 (C-4), 26.8 (C-8'), 26.6 (C-1), 23.2, 21.7 (C-2, C-3); ESI-MS: *m/z* 459.0 [M]⁺ (calculated for: [C₂₉H₃₉N₄O]⁺ 459.3); Anal. Calcd for C₂₉H₄₁Cl₃N₄O: C, 61.32; H, 7.28; N, 9.86 Found: C, 61.45; H, 7.25; N, 10.05.

4.1.4.17. 7-Methoxy-N-{2-[4-(5-phenylpentyl)piperazin-1-yl]ethyl}-1,2,3,4-tetrahydroacridin-9-amine trihydrochloride (20). Yellow solid (0.26 g, 73%); mp = 81.1–84.2 °C; ¹H NMR ((CD₃)₂SO): δ 8.04 (d, 1H, CH, H-5, *J* = 9.2 Hz), 7.86 (s, 1H, CH, H-8), 7.52 (dd, 1H, CH, H-

6, *J* = 9.2, 2.3 Hz), 7.25 (m, 2H, 2 × CH, H-13', H-17'), 7.17 (m, 3H, 3 × CH, H-14', H-15', H-16'), 4.30 (m, 2H, CH₂, H-7'), 3.97 (s, 3H, OCH₃), 3.69 (m, 8H, 4 × CH₂, H-3', H-4', H-5', H-6'), 3.06 (t, 2H, CH₂, H-4, *J* = 6.1 Hz), 2.84 (m, 2H, CH₂, H-1), 2.56 (t, 2H, CH₂, H-11', *J* = 7.6 Hz), 2.50 (m, 4H, 2 × CH₂, H-1', H-2'), 1.78 (m, 6H, 3 × CH₂, H-2, H-3, H-10'), 1.56 (m, 2H, CH₂, H-8'), 1.30 (m, 2H, CH₂, H-9'); ¹³C NMR ((CD₃)₂SO): δ 157.1 (C-10a), 154.9 (C-9), 150.7 (C-4a), 142.2 (C-12'), 132.6 (C-7), 128.5 (C-13', C-14', C-16', C-17'), 125.9 (C-15'), 124.5 (C-6), 121.1 (C-5), 118.2 (C-8a), 112.5 (C-9a), 103.6 (C-8), 56.6 (OCH₃), 55.6 (C-3', C-6'), 48.7 (C-4', C-5'), 41.0 (C-7'), 40.2 (C-1', C-2'), 35.0 (C-11'), 30.5 (C-8'), 28.1 (C-4), 25.7 (C-9'), 25.5 (C-1), 22.5, 22.0 (C-2, C-3), 20.4 (C-10'); ESI-MS: *m/z* 487.0 [M]⁺ (calculated for: [C₃₁H₄₃N₄O]⁺ 487.3); Anal. Calcd for C₃₁H₄₅Cl₃N₄O: C, 62.46; H, 7.61; N, 9.40 Found: C, 62.50; H, 7.77; N, 9.39.

4.1.4.18. 7-Methoxy-N-{2-[4-(naphthalen-2-ylmethyl)piperazin-1-yl]ethyl}-1,2,3,4-tetrahydroacridin-9-amine trihydrochloride (21). Yellow solid (0.28 g, 81%); mp = 164.5–168.8 °C; ¹H NMR (CD₃OD): δ 8.16 (m, 1H, CH, H-16'), 7.98 (d, 1H, CH, H-5, *J* = 9.2 Hz), 7.93 (m, 3H, 3 × CH, H-9', H-10', H-11'), 7.76 (s, 1H, CH, H-8), 7.71 (m, 1H, CH, H-14'), 7.57 (m, 2H, 2 × CH, H-12', H-13'), 7.49 (dd, 1H, CH, H-6, *J* = 9.2, 2.3 Hz), 4.70 (m, 2H, CH₂, H-7'), 4.37 (m, 4H, 2 × CH₂, H-3', H-6'), 4.01 (s, 3H, OCH₃), 3.80 (m, 4H, 2 × CH₂, H-4', H-5'), 3.32 (m, 4H, 2 × CH₂, H-1', H-2'), 3.05 (t, 2H, CH₂, H-4, *J* = 6.0 Hz), 2.89 (t, 2H, CH₂, H-1, *J* = 5.6 Hz), 1.95 (m, 4H, 2 × CH₂, H-2, H-3); ¹³C NMR (CD₃OD): δ 159.3 (C-10a), 156.9 (C-9), 152.1 (C-4a), 135.3 (C-8'), 134.5 (C-9a'), 134.1 (C-13a'), 133.0 (C-15'), 130.4 (C-9', C-10', C-11'), 128.9 (C-12', C-13', C-14'), 128.1 (C-14'), 126.7 (C-6), 126.1 (C-7), 121.9 (C-5), 119.7 (C-8a), 114.6 (C-9a), 104.0 (C-8), 60.8 (C-7'), 57.1 (OCH₃), 50.3 (C-4', C-5'), 48.2 (C-1', C-2'), 42.5 (C-3', C-6'), 29.4 (C-4), 26.7 (C-1), 23.2, 21.7 (C-2, C-3); ESI-MS: *m/z* 481.0 [M]⁺ (calculated for: [C₃₁H₃₇N₄O]⁺ 481.3); Anal. Calcd for C₃₁H₃₉Cl₃N₄O: C, 63.10; H, 6.66; N, 9.50 Found: C, 63.35; H, 6.81; N, 9.47.

4.1.4.19. 7-Methoxy-N-{2-[4-(naphthalen-1-ylmethyl)piperazin-1-yl]ethyl}-1,2,3,4-tetrahydroacridin-9-amine trihydrochloride (22). Yellow solid (0.26 g, 76%); mp = 171.4–174.8 °C; ¹H NMR ((CD₃)₂SO): δ 8.04 (d, 1H, CH, H-5, *J* = 9.2 Hz), 8.00 (m, 4H, 2 × CH, H-9', H-10', H-11', H-15'), 7.83 (s, 1H, CH, H-8), 7.62 (m, 3H, 3 × CH, H-12', H-13', H-14'), 7.50 (dd, 1H, CH, H-6, *J* = 9.2, 2.4 Hz), 4.27 (d, 2H, CH₂, H-7', *J* = 5.3 Hz), 3.96 (s, 3H, OCH₃), 3.70 (m, 8H, 4 × CH₂, H-3', H-4', H-5', H-6'), 3.04 (t, 2H, CH₂, H-4, *J* = 6.0 Hz), 2.81 (m, 2H, CH₂, H-1), 2.49 (m, 4H, 2 × CH₂, H-1', H-2'), 1.78 (m, 4H, 2 × CH₂, H-2, H-3); ¹³C NMR ((CD₃)₂SO): δ 157.1 (C-10a), 154.9 (C-9), 150.7 (C-4a), 133.6 (C-8'), 132.5 (C-11'), 132.3 (C-15a'), 130.6 (C-15'), 128.9 (C-9', C-10', C-11'), 127.2 (C-12', C-13', C-14'), 126.4 (C-7), 124.3 (C-6), 121.0 (C-5), 118.1 (C-8a), 112.3 (C-9a), 103.5 (C-8), 56.6 (OCH₃), 48.6 (C-3', C-4', C-5', C-6'), 41.1 (C-7'), 40.3 (C-1', C-2'), 28.1 (C-4), 25.5 (C-1), 21.9, 20.4 (C-2, C-3); ESI-MS: *m/z* 481.0 [M]⁺ (calculated for: [C₃₁H₃₇N₄O]⁺ 481.3); Anal. Calcd for C₃₁H₃₉Cl₃N₄O: C, 63.10; H, 6.66; N, 9.50 Found: C, 63.29; H, 6.64; N, 9.42.

4.1.4.20. 7-Methoxy-N-{2-[4-[2-(naphthalen-1-yl)ethyl]piperazin-1-yl]ethyl}-1,2,3,4-tetrahydroacridin-9-amine trihydrochloride (23). Yellow solid (0.26 g, 74%); mp = 169.4–170.5 °C; ¹H NMR (CD₃OD): δ 8.16 (d, 1H, CH, H-16', *J* = 8.4 Hz), 7.86 (d, 1H, CH, H-10', *J* = 8.1 Hz), 7.78 (d, 1H, CH, H-5, *J* = 9.2 Hz), 7.74 (s, 1H, CH, H-8), 7.72 (m, 2H, 2 × CH, H-11', H-12'), 7.56 (m, 3H, 3 × CH, H-13', H-14', H-15'), 7.46 (dd, 1H, CH, H-6, *J* = 9.2, 2.3 Hz), 4.40 (t, 2H, CH₂, H-7', *J* = 6.1 Hz), 4.03 (s, 3H, OCH₃), 3.77 (t, 2H, CH₂, H-8', *J* = 6.4 Hz), 3.61 (m, 8H, 4 × CH₂, H-3', H-4', H-5', H-6'), 3.04 (t, 2H, CH₂, H-4, *J* = 6.1 Hz), 2.90 (t, 2H, CH₂, H-1, *J* = 6.1 Hz), 2.49 (m, 4H, 2 × CH₂, H-1', H-2'), 1.93 (m, 4H, 2 × CH₂, H-2, H-3); ¹³C NMR (CD₃OD): δ 159.4 (C-10a), 156.9 (C-9), 152.1 (C-4a), 135.4 (C-9'), 133.9 (C-12a'), 133.0 (C-16a'), 130.0 (C-16'), 129.2 (C-10', C-11', C-12'), 127.8 (C-13', C-14', C-15'), 126.7 (C-

7), 124.3 (C-6), 121.9 (C-5), 119.8 (C-8a), 114.6 (C-9a), 104.0 (C-8), 57.8 (C-7'), 57.2 (OCH₃), 50.5 (C-4', C-5'), 49.6 (C-1', C-2'), 42.3 (C-3', C-6'), 28.3 (C-4), 26.9 (C-1), 23.2, 21.7 (C-2, C-3); ESI-MS: m/z 495.0 [M]⁺ (calculated for: [C₃₂H₃₉N₄O]⁺ 495.3); Anal. Calcd for C₃₂H₄₁Cl₃N₄O: C, 63.63; H, 6.84; N, 9.28 Found: C, 63.42; H, 6.94; N, 9.40.

4.1.4.21. N-{2-[4-(cyclohexylmethyl)piperazin-1-yl]ethyl}-7-methoxy-1,2,3,4-tetrahydroacridin-9-amine trihydrochloride (24). White solid (0.21 g, 65%); mp = 172.8–174.9 °C; ¹H NMR (CD₃OD): δ 7.78 (d, 1H, CH, H-5, *J* = 9.2 Hz), 7.73 (s, 1H, CH, H-8), 7.51 (dd, 1H, CH, H-6, *J* = 9.2, 2.4 Hz), 4.40 (m, 2H, CH₂, H-7'), 4.02 (s, 3H, OCH₃), 3.71 (m, 8H, 4 × CH₂, H-3', H-4', H-5', H-6'), 3.22 (m, 4H, 2 × CH₂, H-1', H-2'), 3.04 (t, 2H, CH₂, H-4, *J* = 6.1 Hz), 2.95 (t, 2H, CH₂, H-1, *J* = 5.7 Hz), 1.98 (m, 4H, 2 × CH₂, H-2, H-3), 1.15 (m, 10H, 5 × CH₂, H-9', H-10', H-11', H-12', H-13'); ¹³C NMR (CD₃OD): δ 159.5 (C-10a), 157.0 (C-9), 152.2 (C-4a), 134.1 (C-7), 126.2 (C-6), 121.9 (C-5), 119.8 (C-8a), 114.7 (C-9a), 104.0 (C-8), 57.2 (OCH₃), 49.5 (C-7'), 50.2 (C-3', C-4', C-5', C-6'), 42.3 (C-1', C-2'), 33.9 (C-9', C-13'), 31.8 (C-8'), 29.4 (C-4), 27.0 (C-11'), 26.8 (C-10', C-12'), 26.4 (C-1), 23.3, 21.7 (C-2, C-3); ESI-MS: m/z 437.0 [M]⁺ (calculated for: [C₂₇H₄₁N₄O]⁺ 437.3); Anal. Calcd for C₂₇H₄₃Cl₃N₄O: C, 59.39; H, 7.94; N, 10.26 Found: C, 59.36; H, 7.88; N, 10.21.

4.1.4.22. 7-Methoxy-N-{2-[4-(prop-2-yn-1-yl)piperazin-1-yl]ethyl}-1,2,3,4-tetrahydroacridin-9-aminetrihydrochloride (25). White solid (0.24 g, 84%); mp = 183.4–185.3 °C; ¹H NMR (D₂O): δ 7.52 (d, 1H, CH, H-5, *J* = 9.2 Hz), 7.40 (dd, 1H, CH, H-6, *J* = 9.2, 2.4 Hz), 7.27 (s, 1H, CH, H-8), 4.89 (m, 4H, 2 × CH₂, H-3', H-6'), 4.40 (m, 2H, CH₂, H-7'), 3.94 (s, 3H, OCH₃), 3.74 (m, 4H, 2 × CH₂, H-4', H-5'), 3.20 (m, 1H, CH, H-8'), 2.97 (m, 2H, CH₂, H-4), 2.71 (m, 2H, CH₂, H-1), 2.21 (m, 4H, 2 × CH₂, H-1', H-2'), 1.88 (m, 4H, 2 × CH₂, H-2, H-3); ¹³C NMR (D₂O): δ 157.4 (C-10a), 155.6 (C-9), 151.6 (C-4a), 132.8 (C-7'), 124.5 (C-6), 121.2 (C-5), 118.3 (C-8a), 114.2 (C-9a), 103.5 (C-8), 71.4 (C-8'), 56.9 (OCH₃), 48.8 (C-4', C-5'), 46.4 (C-3', C-6'), 41.7 (C-1', C-2'), 28.7 (C-4), 25.4 (C-1), 22.2, 20.7 (C-2, C-3); ESI-MS: m/z 379.0 [M]⁺ (calculated for: [C₂₃H₃₁N₄O]⁺ 379.2); Anal. Calcd for C₂₃H₃₃Cl₃N₄O: C, 56.62; H, 6.82; N, 11.48 Found: C, 56.75; H, 6.93; N, 11.35.

4.2. In vitro inhibition studies on AChE and BChE

Multichannel spectrophotometer Sunrise (Tecan, Salzburg, Austria) was used for all measurements of cholinesterase activity. Previously optimized Ellman's procedure was slightly adopted in order to estimate anticholinergic properties [53,54]. 96-wells photometric microplates made from polystyrene (Nunc, Rockville, Denmark) were used for measurement purposes. Human recombinant AChE (hAChE), human plasmatic BChE (hBChE), horse serum BChE (eqBChE) and electric eel AChE (EeAChE) (Aldrich; commercially purified by affinity chromatography) were suspended into phosphate buffer (pH 7.4) up to final activity 0.002 U/μL. Cholinesterase (5 μL), solution of 0.4 mg/mL 5,5'-dithio-bis(2-nitrobenzoic) acid (40 μL), 1 mM acetylthiocholine chloride in phosphate buffer (20 μL) and appropriate concentration of inhibitor (1 mM–0.1 nM; 5 μL) were injected per well. Absorbance was measured at 412 nm after 5 min incubation using automatic shaking of the microplate.

Percentage of inhibition (I) was calculated from the measured data as follows:

$$I = 1 - \frac{\Delta A_i}{\Delta A_0}$$

ΔA_i indicates absorbance change provided by cholinesterase exposed to anticholinergic compound. ΔA₀ indicates absorbance

change caused by intact cholinesterase, where phosphate buffer was applied in the same way as the anticholinergic compound.

IC₅₀ was determined using GraphPad Prism 6 (La Jolla, CA, USA). Percentage of inhibition was overlaid by proper curve chosen according to optimal correlation coefficient. All results are determined as the mean of three independent measurements. Subsequently, IC₅₀ was computed and standard error of the mean was established.

4.3. Kinetic analysis of ChE inhibition

Enzyme inhibition was measured with crude AChE extract prepared from whole rat brain (minus cerebellum) tissue. Extraction was performed in "saline buffer" (10 mM Na–P pH 7.0/1 M NaCl/50 mM MgCl₂ + 1% Triton X-100) [55]. Tissue was homogenized in app. 10 volumes of buffer in Potter-Elvehjem glass-teflon homogenizer, 1200 rpm, 2 × 5 up-down strikes; on ice. Homogenate was then centrifuged at 13 000 rpm/30 min/4 °C in Beckman J2-HS, the supernatant aliquoted, frozen and kept at –40 °C (not longer than 4 weeks). Preparation used for AChE activity measurements was thawed just once. All chemicals were of p.a. purity, purchased from Sigma–Aldrich.

AChE activities were assayed by the spectrophotometric method according to Ellman et al. (with minor modifications) [53]. Measurements were performed with Shimadzu 2101 PC spectrophotometer at 412 nm and ambient temperature (cca 21–23 °C), as duplicates or triplicates in final volume of 1 mL, with following final concentrations: 100 mM Na-phosphate pH 8.0/100 mM NaCl/5 mM MgCl₂/0.1% Triton X-100/0.5 mM DTNB, varying concentrations of ATCh (0.1–0.8 mM) and of the inhibitors (at 6–8 serial dilutions, usually at low to high micromolar range). Absorbance was recorded electronically at 2 readings for 2 min continuously; reaction started with addition of substrate (ATCh) into premixed enzyme/buffer/inhibitor mixture. Final enzyme activity used for assay was in the range of 10–15 nmol/min. Reaction mixture without enzyme preparation served as a blank. For measured intervals, enzyme rates were always linear (can be considered as the initial rates). Measured data were analyzed by GraphPad Prism software. For enzyme rate calculation, molar extinction coefficient 13 600 for DTNB was considered.

K_i calculations were derived from Dixon plot; linear transformation of reciprocal enzyme rates vs. inhibitor concentrations (Fig. 4, Table 2) [43].

As the Dixon plot cannot distinguish between competitive and mixed inhibitors, Cornish–Bowden transformation (S/V_i vs. inhibitor concentrations, Fig. 3) was used for definitive identification of the type of inhibition [42].

4.4. Molecular modeling studies

From the online PDB database (www.pdb.org) models of hAChE (PDB ID: 4EY7, resolution: 2.35 Å), hBChE (PDB ID: 4BDS, resolution: 2.10 Å) and EeAChE (PDB ID: 1C2O, resolution: 4.2 Å) were downloaded and prepared for flexible molecular docking by MGL Tools utilities [56]. An appropriate structure model of eqBChE was not available from the database. The preparation of these receptors involved removing surplus copies of the enzyme chains, non-bonded inhibitors and water molecules, addition of polar hydrogens and merging non-polar ones. Default Gasteiger charges were assigned to all atoms. The flexible parts of the enzymes were determined by a spherical selection of residues (*R* = 11 Å) approximately around the middle of the active site. In the same points the centers of the grid boxes of 33 × 33 × 33 Å were positioned. The rotatable bonds in the flexible residues were detected automatically by AutoDock Tools 1.5.4 program. The flexible

receptor parts contained 40 residues for hAChE, 39 residues for hBChE and 34 residues for EeAChE. Following xyz coordinates of the grid box centers were applied: hAChE (10.698, –58.115, –23.192), hBChE (140.117, 122.247, 38.986), EeAChE (45.094, 68.205, –80.941). The ligands under the study were firstly drawn in HyperChem 7.52, then manually protonated as suggested by MarvinSketch 6.2.0. software (<http://www.chemaxon.com>), geometrically optimized by semi-empirical quantum-chemistry PM3 method and stored as pdb files. The structures of the ligands were processed for docking in a similar way as above mentioned flexible parts of the receptors by AutoDock Tools 1.5.4 program, with the exception that we used directly the prepare_ligand4.py script of MGL Tools with default setting. Molecular docking was carried out in AutoDock Vina 1.1.2 program utilizing computer resources of Czech National Grid Infrastructure MetaCentrum [46]. The search algorithm of AutoDock Vina efficiently combines a Markov chain Monte Carlo like method for the global search and a Broyden–Fletcher–Goldfarb–Shanno gradient approach for the local search [46]. It is a type of memetic algorithm based on interleaving stochastic and deterministic calculations [57]. Each docking task was repeated 5 times with the exhaustiveness parameter set to 16, employing 16 CPU in parallel multithreading. The means, sample standard deviations (SD) and charts were prepared in Microsoft Excel 2007. The graphic representations of the docked poses were rendered in PyMOL 1.3 [49].

Acknowledgments

The work was supported by the Grant Agency of the Czech Republic (No. P303/11/1907), by Post-doctoral project (No. CZ.1.07/2.3.00/30.0044), by University of Defence (Long Term Development Plan – 1011), by MH CZ – DRO (University Hospital Hradec Kralove, No. 00179906), by MH CZ – DRO (PCP, No 00023752), by University of Hradec Kralove (Long Term Development Plan) and by the grant of the Ministry of Education, Youth and Sports of the Czech Republic (No. SVV-260-062). The access to computing and storage facilities owned by parties and projects contributing to the National Grid Infrastructure MetaCentrum, provided under the program "Projects of Large Infrastructure for Research, Development, and Innovations" (LM2010005) is highly appreciated.

Appendix A. Supplementary data

Supplementary data related to this article can be found at <http://dx.doi.org/10.1016/j.ejmech.2014.05.066>.

References

- [1] T. Fukami, T. Yokoi, The emerging role of human esterases, *Drug Metab. Pharmacokinet.* 27 (2012) 466–477.
- [2] Chatonnet, O. Lockridge, Comparison of butyrylcholinesterase and acetylcholinesterase, *Biochem. J.* 260 (1989) 625–634.
- [3] X. Sun, L. Jin, P. Ling, Review of drugs for Alzheimer's disease, *Drug Discov. Ther.* 6 (2012) 285–290.
- [4] D. Lo, G.T. Grossberg, Use of memantine for the treatment of dementia, *Expert Rev. Neurother.* 11 (2011) 1359–1370.
- [5] E.D. Roberson, L. Mucke, 100 years and counting: prospects for defeating Alzheimer's disease, *Science* 314 (2006) 781–784.
- [6] J. Korabecny, F. Zemek, O. Soukup, K. Spilovska, K. Musilek, D. Jun, E. Nepovimova, K. Kuca, Current treatment and perspectives in pharmacotherapy of Alzheimer's disease, *Front. Drug Des. Discov.* 6 (2014) 702–738.
- [7] H.O. Tayeb, E.D. Murray, B.H. Price, F.I. Tarazi, Bapineuzumab and solanezumab for Alzheimer's disease: is the 'amyloid cascade hypothesis' still alive? *Expert Opin. Biol. Ther.* 13 (2013) 1075–1084.
- [8] R. León, A.G. García, J. Marco-Contelles, Recent advances in the multitarget-directed ligands approach for the treatment of Alzheimer's disease, *Med. Res. Rev.* 33 (2013) 139–189.
- [9] J. Patocka, D. Jun, K. Kuca, Possible role of hydroxylated metabolites of tacrine in drug toxicity and therapy of Alzheimer's disease, *Curr. Drug Metab.* 9 (2008) 332–335.
- [10] V. Tumiatti, A. Minarini, M.L. Bolognesi, A. Milelli, M. Rosini, C. Melchiorre, Tacrine derivatives and Alzheimer's disease, *Curr. Med. Chem.* 17 (2010) 1825–1838.
- [11] J. Patocka, J. Bielavsky, J. Fusek, Advances in synthesis of tacrine derivatives as potential-drugs for treatment of Alzheimer's disease, *Homeost. Health Dis.* 35 (1994) 299–301.
- [12] J. Patocka, J. Bajgar, J. Bielavsky, J. Fusek, Kinetics of inhibition of cholinesterases by 1,2,3,4-tetrahydro-9-aminoacridine in vitro, *Collect. Czech Chem. Commun.* 41 (1976) 816–824.
- [13] L. Dejmeck, 7-MEOTA, *Drug Future* 15 (1990) 126–129.
- [14] H. Sugimoto, Y. Tsuchiya, H. Sugumi, K. Higurashi, N. Karibe, Y. Limura, A. Sasaki, Y. Kawakami, T. Nakamura, S. Araki, Y. Yamanishi, K. Yamatsu, Novel piperidine derivatives. Synthesis and anti-acetylcholinesterase activity of 1-benzyl-4-[2-(N-benzoylamino)ethyl]piperidine derivatives, *J. Med. Chem.* 33 (1990) 1880–1881.
- [15] R.S. Doody, J.L. Cummings, M.R. Farlow, Reviewing the role of donepezil in the treatment of Alzheimer's disease, *Curr. Alzheimer Res.* 9 (2012) 773–781.
- [16] J. Cheung, M.J. Rudolph, F. Burshteyn, M.S. Cassidy, E.N. Gary, J. Love, M.C. Franklin, J.J. Height, Structures of human acetylcholinesterase in complex with pharmacologically important ligands, *J. Med. Chem.* 55 (2012) 10282–10286.
- [17] K. Spilovska, J. Korabecny, J. Kral, A. Horova, K. Musilek, O. Soukup, L. Drtinova, Z. Gazova, K. Siposova, K. Kuca, 7-Methoxytacrine-adamantylamine heterodimers as cholinesterase inhibitors in Alzheimer's disease treatment—synthesis, biological evaluation and molecular modeling studies, *Molecules* 18 (2013) 2397–2418.
- [18] Cavalli, M.L. Bolognesi, A. Minarini, M. Rosini, V. Tumiatti, M. Recanatini, C. Melchiorre, Multi-target-directed ligands to combat neurodegenerative diseases, *J. Med. Chem.* 51 (2008) 347–372.
- [19] N.C. Inestrosa, A. Alvarez, C.A. Pérez, R.D. Moreno, M. Vicente, C. Linker, O.I. Casanueva, C. Soto, J. Garrido, Acetylcholinesterase accelerates assembly of amyloid-beta-peptides into Alzheimer's fibrils: possible role of the peripheral site of the enzyme, *Neuron* 16 (1996) 881–891.
- [20] Y.P. Pang, P. Quiram, T. Jelacic, F. Hong, S. Brimijoin, Highly potent, selective, and low cost bis-tetrahydroaminacrine inhibitors of acetylcholinesterase. Steps toward novel drugs for treating Alzheimer's disease, *J. Biol. Chem.* 271 (1996) 23646–23649.
- [21] Badia, J.E. Baños, P. Camps, J. Contreras, D.M. Görbig, D. Muñoz-Torrero, M. Simón, N.M. Vivas, Synthesis and evaluation of tacrine-huperzine A hybrids as acetylcholinesterase inhibitors of potential interest for the treatment of Alzheimer's disease, *Bioorg. Med. Chem.* 6 (1998) 427–440.
- [22] P. Muñoz-Ruiz, L. Rubio, E. García-Palomero, I. Dorronsoro, M. del Monte-Millán, R. Valenzuela, P. Usán, C. de Austria, M. Bartolini, V. Andrisano, A. Bidon-Chanal, M. Orozco, F.J. Luque, M. Medina, A. Martínez, Design, synthesis, and biological evaluation of dual binding site acetylcholinesterase inhibitors: new disease-modifying agents for Alzheimer's disease, *J. Med. Chem.* 48 (2005) 7223–7233.
- [23] M.I. Fernández-Bachiller, C. Pérez, L. Monjas, J. Rademann, M.I. Rodríguez-Franco, New tacrine-4-oxo-4H-chromene hybrids as multifunctional agents for the treatment of Alzheimer's disease, with cholinergic, antioxidant, and β -amyloid-reducing properties, *J. Med. Chem.* 55 (2012) 1303–1317.
- [24] M.L. Bolognesi, V. Andisano, M. Bartolini, R. Banzi, C. Melchiorre, Propidium-based polyamine ligands as potent inhibitors of acetylcholinesterase and acetylcholinesterase-induced amyloid-beta aggregation, *J. Med. Chem.* 48 (2005) 24–27.
- [25] J. Korabecny, K. Musilek, F. Zemek, A. Horova, O. Holas, E. Nepovimova, V. Opletalova, J. Hroudova, Z. Fisar, Y.S. Jung, K. Kuca, *Bioorg. Med. Chem. Lett.* 21 (2011) 6563–6566.
- [26] J. Korabecny, K. Musilek, O. Holas, J. Binder, F. Zemek, J. Marek, M. Pohanka, V. Opletalova, V. Dohnal, K. Kuca, Synthesis and in vitro evaluation of N-alkyl-7-methoxytacrine hydrochlorides as potential cholinesterase inhibitors in Alzheimer disease, *Bioorg. Med. Chem. Lett.* 20 (2010) 6093–6095.
- [27] O. Soukup, D. Jun, J. Zdarova-Karasova, J. Patocka, K. Musilek, J. Korabecny, J. Krusek, M. Kaniakova, V. Sepsova, J. Mandikova, F. Trejtnar, M. Pohanka, L. Drtinova, M. Pavlik, G. Tobin, K. Kuca, A resurrection of 7-MEOTA: a comparison with tacrine, *Curr. Alzheimer Res.* 10 (2013) 893–906.
- [28] E.H. Rydberg, B. Brumshtein, H.M. Greenblatt, D.M. Wong, D. Shaya, L.D. Williams, P.R. Carlier, Y.P. Pang, I. Silman, J.L. Sussman, Complexes of alkylene-linked tacrine dimers with Torpedo californica acetylcholinesterase: binding of Bis5-tacrine produces a dramatic rearrangement in the active-site gorge, *J. Med. Chem.* 49 (2006) 5491–5500.
- [29] Wiecekowska, M. Bajda, N. Guziar, B. Malawska, Novel alkyl- and arylcarbamate derivatives with N-benzylpiperidine and N-benzylpiperazine moieties as cholinesterases inhibitors, *Eur. J. Med. Chem.* 45 (2010) 5602–5611.
- [30] Z. Omran, S. Stiebing, A.M. Godard, J. Sopkova-De Oliveira-Santos, P. Dallemagne, Synthesis and biological evaluation of new donepezil-like thiandianones as AChE inhibitors, *J. Enzyme Inhib. Med. Chem.* 23 (2008) 696–703.
- [31] H. Sugimoto, Y. Yamanishi, Y. Iimura, Y. Kawakami, Donepezil hydrochloride (E 2020) and other acetylcholinesterase inhibitors, *Curr. Med. Chem.* 7 (2000) 303–339.
- [32] D. Alonso, I. Dorronsoro, L. Rubio, P. Muñoz, E. García-Palomero, M. Del Monte, A. Bidon-Chanal, M. Orozco, F.J. Luque, A. Castro, M. Medina, A. Martínez, Donepezil–tacrine hybrid related derivatives as new dual binding site inhibitors of AChE, *Bioorg. Med. Chem.* 13 (2005) 6588–6597.

- [33] M.R. Del Giudice, A. Borioni, C. Mustaza, F. Gatta, A. Meneguz, M.T. Volpe, Synthesis and cholinesterase inhibitory activity of 6-, 7-methoxy- (and hydroxy-) tacrine derivatives, *Farmaco* 51 (1996) 693–698.
- [34] Z. Omran, T. Cailly, E. Lescot, J.S. Santos, J.H. Agondanou, V. Lisowski, F. Fabis, A.M. Godard, S. Stiebing, G. Le Flem, M. Boulouard, F. Dauphin, P. Dallemagne, S. Rault, Synthesis and biological evaluation as AChE inhibitors of new indanones and thiaindanones related to donepezil, *Eur. J. Med. Chem.* 40 (2005) 1222–1245.
- [35] M.M. Ismail, M.M. Kamel, L.W. Mohamed, S.I. Faggal, M.A. Galal, Synthesis and biological evaluation of thiophene derivatives as acetylcholinesterase inhibitors, *Molecules* 17 (2012) 7217–7231.
- [36] M.M. Ismail, M.M. Kamel, L.W. Mohamed, S.I. Faggal, Synthesis of new indole derivatives structurally related to donepezil and their biological evaluation as acetylcholinesterase inhibitors, *Molecules* 17 (2012) 4811–4823.
- [37] Bolea, J. Juárez-Jiménez, C. de Los Ríos, M. Chioua, R. Pouplana, F.J. Luque, M. Unzeta, J. Marco-Contelles, A. Samadi, Synthesis, biological evaluation, and molecular modeling of donepezil and N-[(5-(benzyloxy)-1-methyl-1H-indol-2-yl)methyl]-N-methylprop-2-yn-1-amine hybrids as new multipotent cholinesterase/monoamine oxidase inhibitors for the treatment of Alzheimer's disease, *J. Med. Chem.* 54 (2011) 8251–8270.
- [38] O.M. Bautista-Aguilera, G. Esteban, I. Bolea, K. Nikolic, D. Agbaba, I. Moraleda, I. Iriepa, A. Samadi, E. Soriano, M. Unzeta, J. Marco-Contelles, Design, synthesis, pharmacological evaluation, QSAR analysis, molecular modeling and ADMET of novel donepezil-indolyl hybrids as multipotent cholinesterase/monoamine oxidase inhibitors for the potential treatment of Alzheimer's disease, *Eur. J. Med. Chem.* 75 (2014) 82–95.
- [39] P. Camps, X. Formosa, C. Galdeano, T. Gómez, D. Muñoz-Torrero, M. Scarpellini, E. Viayna, A. Badia, M.V. Clos, A. Camins, M. Pallàs, M. Bartolini, F. Mancini, V. Andrisano, J. Estelrich, M. Lizondo, A. Bidon-Chanal, F.J. Luque, Novel donepezil-based inhibitors of acetyl- and butyrylcholinesterase and acetylcholinesterase-induced β -amyloid aggregation, *J. Med. Chem.* 51 (2008) 3588–3598.
- [40] P. Camps, X. Formosa, C. Galdeano, T. Gómez, D. Muñoz-Torrero, L. Ramírez, E. Viayna, E. Gómez, N. Isambert, R. Lavilla, A. Badiad, M.V. Clos, M. Bartolini, F. Mancini, V. Andrisano, A. Bidon-Chanal, O. Huertas, T. Dafnif, F.J. Luque, Tacrine-based dual binding site acetylcholinesterase inhibitors as potential disease-modifying anti-Alzheimer drug candidates, *Chem. Biol. Interact.* 187 (2010) 411–415.
- [41] E. Viayna, T. Gómez, C. Galdeano, L. Ramírez, M. Ratia, A. Badia, M.V. Clos, E. Verdager, F. Junyent, A. Camins, M. Pallàs, M. Bartolini, F. Mancini, V. Andrisano, M.P. Arce, M.I. Rodríguez-Franco, A. Bidon-Chanal, F.J. Luque, P. Camps, D. Muñoz-Torrero, Novel huprine derivatives with inhibitory activity toward β -amyloid aggregation and formation as disease-modifying anti-Alzheimer drug candidates, *ChemMedChem* 5 (2010) 1855–1870.
- [42] A. Cornish-Bowden, A simple graphical method for determining the inhibition constants of mixed, uncompetitive and non-competitive inhibitors, *Biochem. J.* 137 (1974) 143–144.
- [43] M. Dixon, The determination of enzyme inhibitor constants, *Biochem. J.* 55 (1953) 170–171.
- [44] F. Nachon, E. Carletti, C. Ronco, M. Trovaslet, Y. Nicolet, L. Jean, P. Renard, Crystal structures of human cholinesterases in complex with huprine W and tacrine: elements of specificity for anti-Alzheimer's drugs targeting acetyl- and butyryl-cholinesterase, *Biochem. J.* 453 (2013) 393–399.
- [45] Y. Bourne, J. Grassi, P.E. Bougis, P. Marchot, Conformational flexibility of the acetylcholinesterase tetramer suggested by x-ray crystallography, *J. Biol. Chem.* 274 (1999) 30370–30376.
- [46] O. Trott, A.J. Olson, Software news and update AutoDock Vina: Improving the speed and accuracy of docking with a new scoring function, efficient optimization, and multithreading, *J. Comput. Chem.* 31 (2010) 455–461.
- [47] ChemAxon, <http://www.chemaxon.com>.
- [48] S.K. Panigrahi, G.R. Desiraju, Strong and weak hydrogen bonds in the protein–ligand interface, *Proteins* 67 (2007) 128–141.
- [49] The PyMOL Molecular Graphics System, Version 1.5.0.4, Schrödinger, LLC.
- [50] W. Luo, Y.-P. Li, Y. He, S.-L. Huang, D. Li, L.-Q. Gu, Z.-S. Huang, Synthesis and evaluation of heterobivalent tacrine derivatives as potential multi-functional anti-Alzheimer agents, *Eur. J. Med. Chem.* 46 (2011) 2609–2616.
- [51] J.S. da Costa, J.P. Lopes, D. Russowsky, C.L. Petzhold, A.C. Borges, M.A. Ceschi, E. Konrath, C. Batassini, P.S. Lunardi, C.A. Gonçalves, Synthesis of tacrine-ophine hybrids via one-pot four component reaction and biological evaluation as acetyl- and butyrylcholinesterase inhibitors, *Eur. J. Med. Chem.* 62 (2013) 556–563.
- [52] S.Y. Li, X.B. Wang, S.S. Xie, N. Jiang, K.D. Wang, H.Q. Yao, H.B. Sun, L.Y. Kong, Multifunctional tacrine-flavonoid hybrids with cholinergic, β -amyloid-reducing, and metal chelating properties for the treatment of Alzheimer's disease, *Eur. J. Med. Chem.* 69 (2013) 632–646.
- [53] G.L. Ellman, D.K. Courtney, V. Andres, R.M. Featherstone, A new and rapid colorimetric determination of acetylcholinesterase activity, *Biochem. Pharmacol.* 7 (1961) 88–95.
- [54] M. Pohanka, J.Z. Karasova, K. Kuca, J. Pikula, O. Holas, J. Korabecny, J. Cabal, Colorimetric dipstick for assay of organophosphate pesticides and nerve agents represented by paraoxon, sarin and VX, *Talanta* 81 (2010) 621–624.
- [55] S. Bon, M. Vigny, J. Massoulié, Asymmetric and globular forms of acetylcholinesterase in mammals and birds, *Proc. Natl. Acad. Sci. U. S. A.* 76 (1979) 2546–2550.
- [56] G.M. Morris, R. Huey, W. Lindstrom, M.F. Sanner, R.K. Belew, D.S. Goodsell, A.J. Olson, Autodock4 and AutoDockTools4: automated docking with selective receptor flexibility, *J. Comput. Chem.* 16 (2009) 2785–2791.
- [57] B. Liu, L. Wang, Y.H. Jin, An effective PSO-based memetic algorithm for flow shop scheduling, *IEEE Trans. Syst. Man. Cybern. B Cybern.* 37 (2007) 18–27.